


OCEAN RESOURCES INVESTIGATION
IN THE SEA AREA OF SOPAC
REPORT ON THE JOINT BASIC STUDY
FOR THE DEVELOPMENT OF RESOURCES

(VOLUME 5)

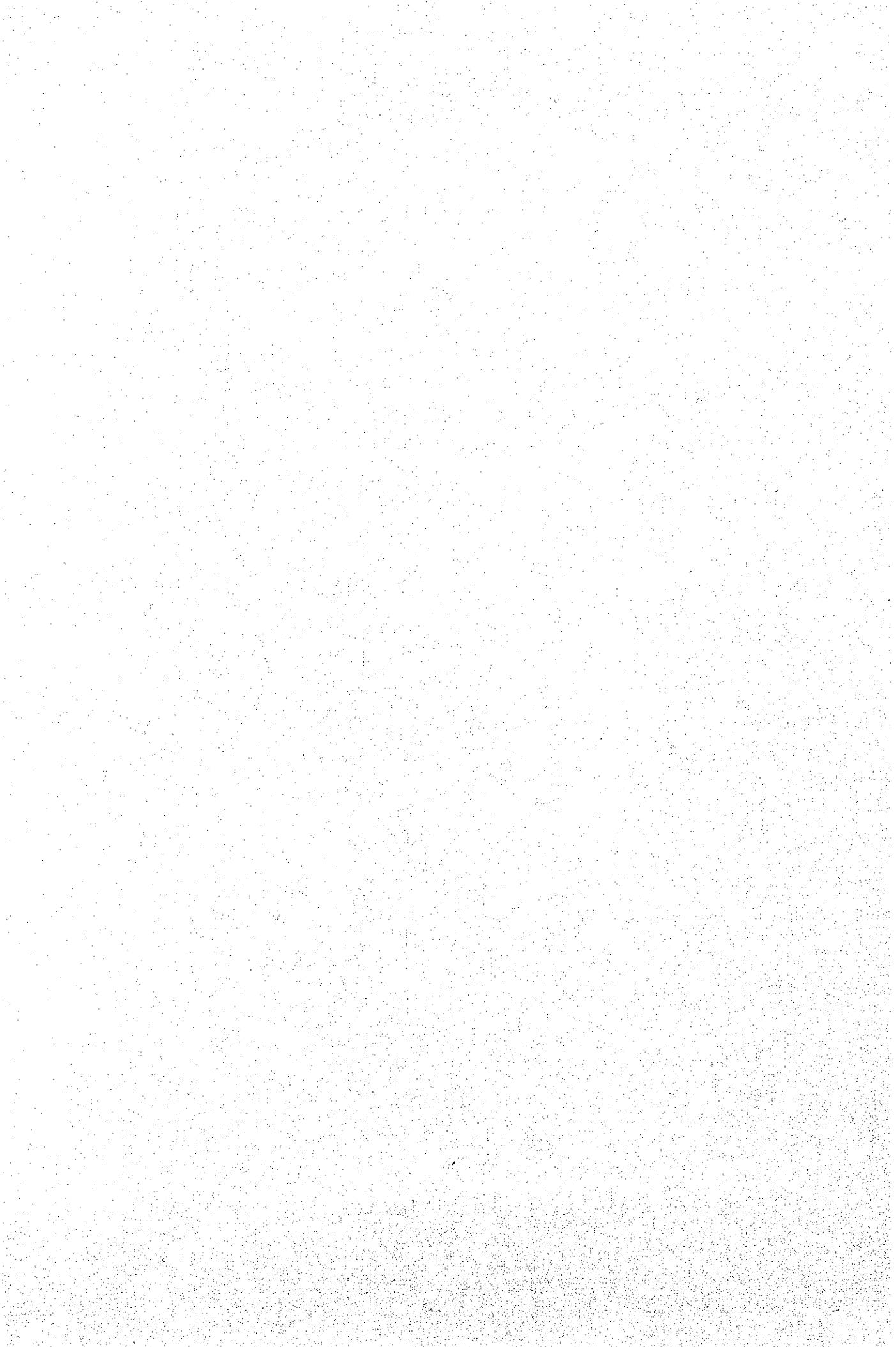
SEA AREA OF REPUBLIC OF VANUATU

March 1995

JICA LIBRARY

J 1127751 (4)

JAPAN INTERNATIONAL COOPERATION AGENCY
METAL MINING AGENCY OF JAPAN

MPN
CR(4)
95-061



**OCEAN RESOURCES INVESTIGATION
IN THE SEA AREA OF SOPAC
REPORT ON THE JOINT BASIC STUDY
FOR THE DEVELOPMENT OF RESOURCES**

(VOLUME 5)

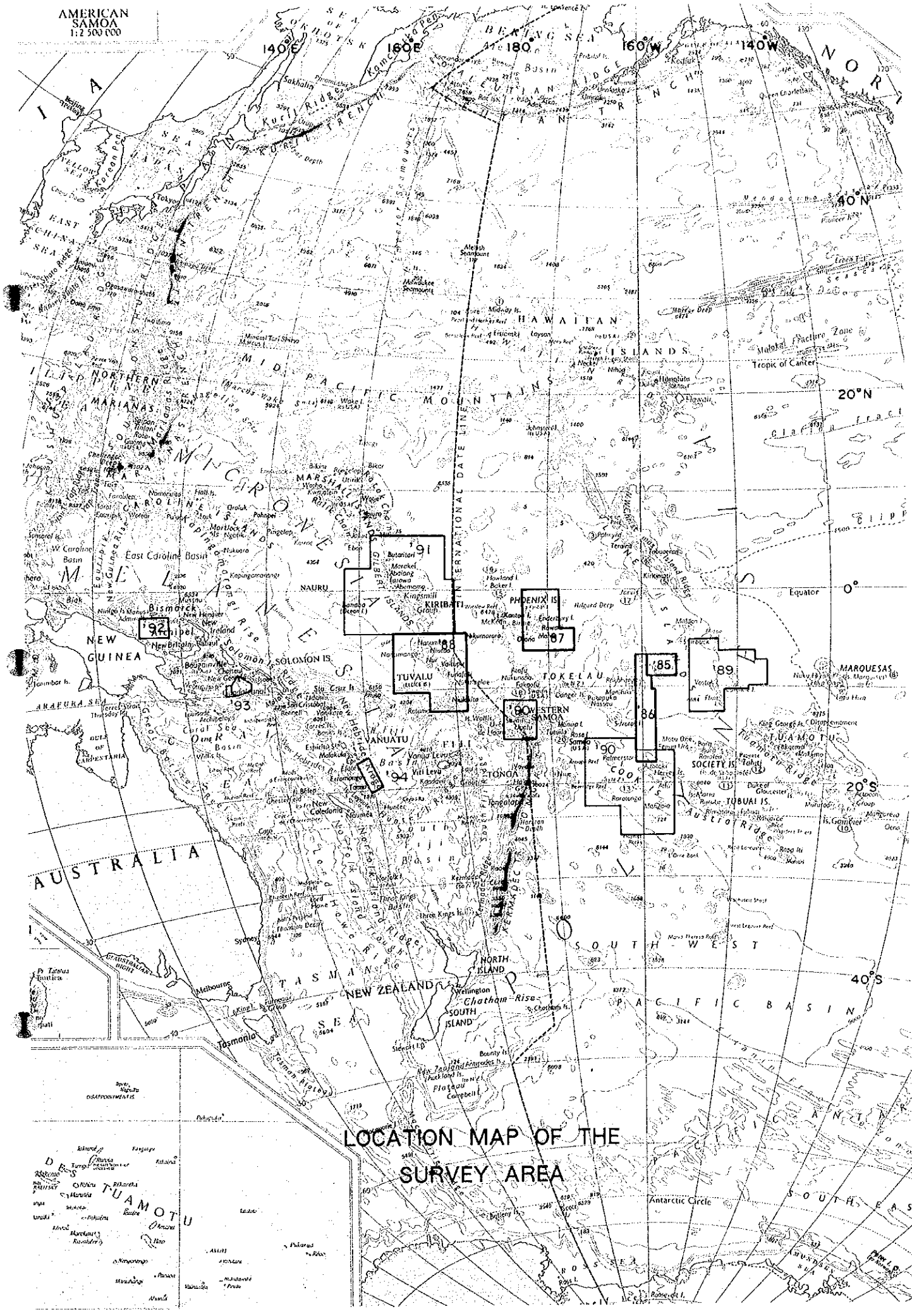
SEA AREA OF REPUBLIC OF VANUATU

March 1995

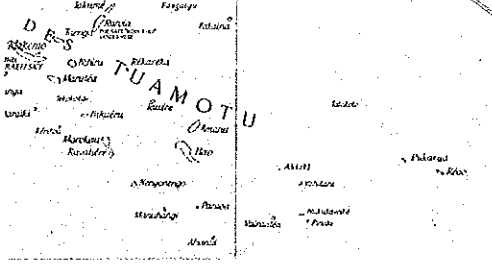
**JAPAN INTERNATIONAL COOPERATION AGENCY
METAL MINING AGENCY OF JAPAN**

1127751【4】

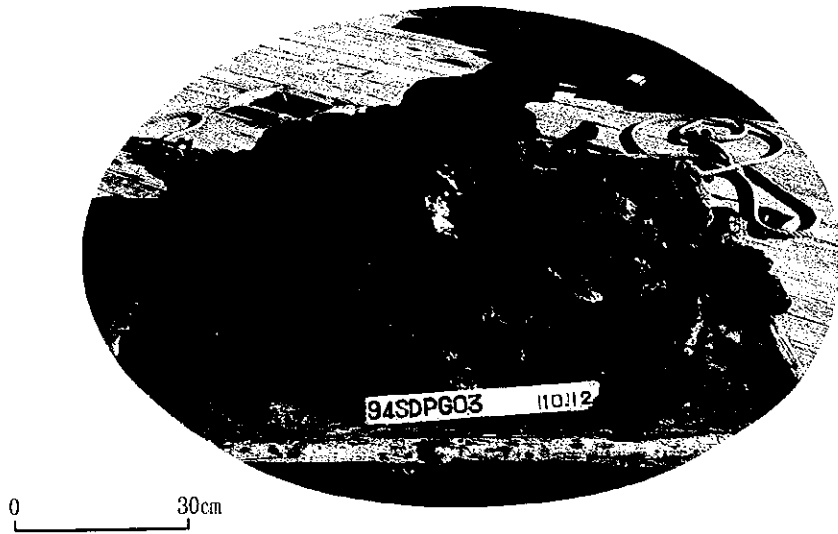
マイクロ
フィルム作成



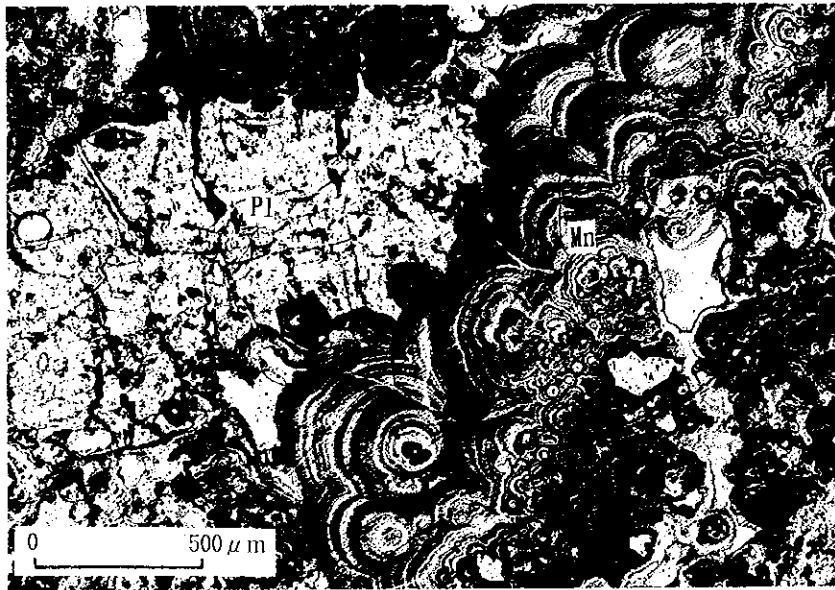
LOCATION MAP OF THE
SURVEY AREA







Manganese oxides collected from 94SDPG03



Reflecting microscopic photo of manganese oxides collected from 94SDPG03

Abbreviation : Pl ; plagioclase, Mn ; birnessite · todorokite

PREFACE

In response to a request by the South Pacific Applied Geoscience Commission (SOPAC), the Government of Japan has undertaken marine geological and other studies relating to mineral prospecting to assess the mineral resource potential of the deep sea bottom in offshore regions of SOPAC member countries. Implementation of the survey has been consigned to the Japan International Cooperation Agency (JAICA). Considering the technical nature of geological and mineral prospecting studies, JICA commissioned the Metal Mining Agency of Japan (MMAJ) to execute the survey.

The survey has been undertaken over a five year period starting from fiscal 1990. The subject of the final, fifth year survey is within the exclusive economic zone of the Republic of Vanuatu.

MMAJ dispatched the Hakurei Maru No.2, a research vessel fitted for investigating deep sea bottom mineral resources, to the sites for a total of 66 days, from August 22, 1994 until October 25, 1994, successfully completing the survey on schedule with the cooperation of the government of the Republic of Vanuatu.

The present report sums up the results of this fifth year survey.

We wish to extend our sincere thanks to all persons concerned, especially for the cooperation given to us by the Secretariat of SOPAC, the Government of the Republic of Vanuatu, as well as the Ministry of Foreign Affairs, the Ministry of International Trade and Industry and the Japanese Embassy in Fiji.

March, 1995.



Kimio Fujita

President

Japan International Cooperation Agency



Takashi Ishikawa

President

Metal Mining Agency of Japan

ABSTRACT

The cooperative basic survey for the development of resources of SOPAC member countries had been scheduled for implementation for five years starting from 1990, and this is its last fiscal year. The survey was implemented from August 22, 1994 to October 25, 1994 on a sea area of about 37,000km² (west of the North Fiji Basin) within the exclusive economic zone of the Republic of Vanuatu. The duration of the survey on the site was 45 days and the target mineral resources were submarine hydrothermal ore deposits.

A regional survey was implemented during the first half of the schedule (Leg 1), during which a topographical survey was conducted for every 2 miles and bathymetric maps were made. Furthermore, in order to help estimate geological structure, a magnetic survey was implemented simultaneously.

Based on the results of the topographical survey and magnetic survey, areas for conducting a mineral deposit survey were selected, submarine observation by FDC and SSS surveys were carried out, and concentrated sampling was carried out at altered zones, districts with hydrothermal biotic communities and mound-shaped rises that had already been observed. A base-line geochemical exploration was also carried out with the object of determining geochemical properties of sediments as a background.

As a result of the topographical survey, the entire aspect of the Coriolis Troughs, which was developing in the direction of NNW~ SSE roughly in the central part of this sea area, was brought to light and several topographic forms suggesting tectonic movement were identified. The characteristics of the Coriolis Troughs are that the inner part of the Coriolis Troughs is divided into three, a small-scaled trough, a basin and others, and that the cliffs on both sides of the Coriolis Troughs are steep, especially, the east cliffs incline steeply and water depths increase gradually toward south.

We found that the acoustic reflection image drawn up using sound pressure received by MBES proved to be an effective method for identifying the distribution of sediments and the submarine situation. These image proved to be effective data for the selection of FDC survey points.

As for magnetic distribution, the whole area appears to be a region of magnetic tranquility. Every magnetic anomaly detected in the northeastern part of the area is small-scaled, except for prominent magnetic anomalies, trending NW-SW.

Based on the bathymetric maps and other data, we paid particular attention to

- ridge topography and sea knolls in the Back Basin
- Seamounts concomitant with tectonic lines in the neighborhood of volcanic fronts, and seamounts and sea knolls with craters
- regions with outcropping rocks or magnetic anomalies appearing to be new volcanic activities and selected the areas for the mineral deposit survey.

By the SSS survey carried out at a portion of apparent indication of mineralization and altered zones, mound-shaped rises promising the generation of hydrothermal mineral deposits were identified and useful information for establishing sampling points was obtained.

Mingling of abundant volcanic elastics in the sediments sampled was recognized by the base-line geochemical survey, which shows that this sea area is an area of active volcanic activities.

Ore indications of mineralization and altered zones were observed relatively extensively during the FDC survey. Total 31 rounds of sampling using FPG, LC and CB were carried out on three areas among those areas with ore indications and altered zones. As a result, reddish brown precipitates appearing to contain iron oxides and crusty manganese oxides, a few centimeters thick, appearing to be hydrothermal were collected from several places, but we could not identify sulphide minerals.

From the above, we found that the ore indications occurring in this sea area existed around ridges and seamounts with structural controls. We were not able to identify sulphide mineral deposits by this year's survey. Even if sulphide mineral deposits exist, they must be oxidized or occurring at lower levels.

At any rate, ore indications and altered zones were observed relatively extensively throughout the sea area. Putting all the results together, we can presume a significant level of hydrothermal activity in this area.

Contents

	Page
Photogravure	
Preface	
Abstract	
Chapter 1. Outline of the Survey	1
1-1 Survey Title	1
1-2 Purpose of the Survey	1
1-3 Survey Area	1
1-4 Term of the Survey	3
1-5 Survey Participants	3
1-6 Survey Apparatus and Equipment	4
1-7 Survey Achievements	4
Chapter 2. Survey Methods	8
2-1 Survey Procedures	8
2-2 Numbering	10
2-3 Ship Positioning and Positioning of Towed Vehicle	10
2-4 Acoustic Soundings	11
2-5 Magnetic Survey (PGM Survey)	11
2-6 Seafloor Observation and Photography	11
2-7 Sampling	13
2-8 CTD Survey	13
2-9 Processing and Analysis of Survey Data	13
Chapter 3. Seafloor Topography and Geological Structure	21
3-1 Outline of the Survey Area	21
3-2 Submarine Topography	22
3-3 Magnetic Survey	27
(1) Total Magnetic Force	27

(2) Magnetic Anomalies	27
(3) Reduction to the Pole Anomalies	33
(4) Magnetization Distribution	35
(5) Magnetic Structure	39
3-4 Geological Structure	41
(1) Geological Structure	41
(2) MBES Acoustic Reflection Image	45
(3) Sub-Bottom Profiling	47
Chapter 4. Baseline Geochemical Survey	51
4-1 Outline	51
4-2 Characteristics of Samples Collected	53
4-3 Results of the Survey	88
(1) Chemical Analysis	88
(2) X-ray Diffraction	89
(3) Statistical Analysis	91
Chapter 5. Ore Deposit Investigation	93
5-1 Outline	93
5-2 FDC Survey	99
5-3 SSS Survey	110
5-4 Characteristics of Samples Collected	114
5-5 Ore Indications	136
5-6 Temperature Anomalies	147
Chapter 6. Discussions	155
Chapter 7. Summary	161

[References]

[Appendix]

1. Sampling Results of the Baseline Geochemical Survey
2. Results of the FDC Observation
3. List of the Ore Indications
4. Sampling Results of the Ore Deposit Investigation (1), (2)
5. List of Samples (1) ~ (4)
6. Results of Chemical Analysis for Sampling Sediments (1) ~ (4)
7. Results of Microscopic Observation (1), (2)
8. Results of X-ray Diffraction Analysis (1), (2)
9. Sea-water Sound Velocity for MBES
10. Weather and Sea-state Data

[List of Annexed Figures]

- Annexed Figure 1 Bathymetric Map
- Annexed Figure 2 Sampling Station of Ore Deposit Investigation (1) ~ (4)
- Annexed Figure 3 Schematic Drawing of Sampling Results Obtained from
Ore Deposit Investigation (1) ~ (3)
- Annexed Figure 4 FDC Route Map (1) ~ (11)
- Annexed Figure 5-1 MBES Track Line Map
- Annexed Figure 5-2 PGM Track Line Map
- Annexed Figure 5-3 SSS Vehicle Position Map (1), (2)

[List of Inserted Figures]

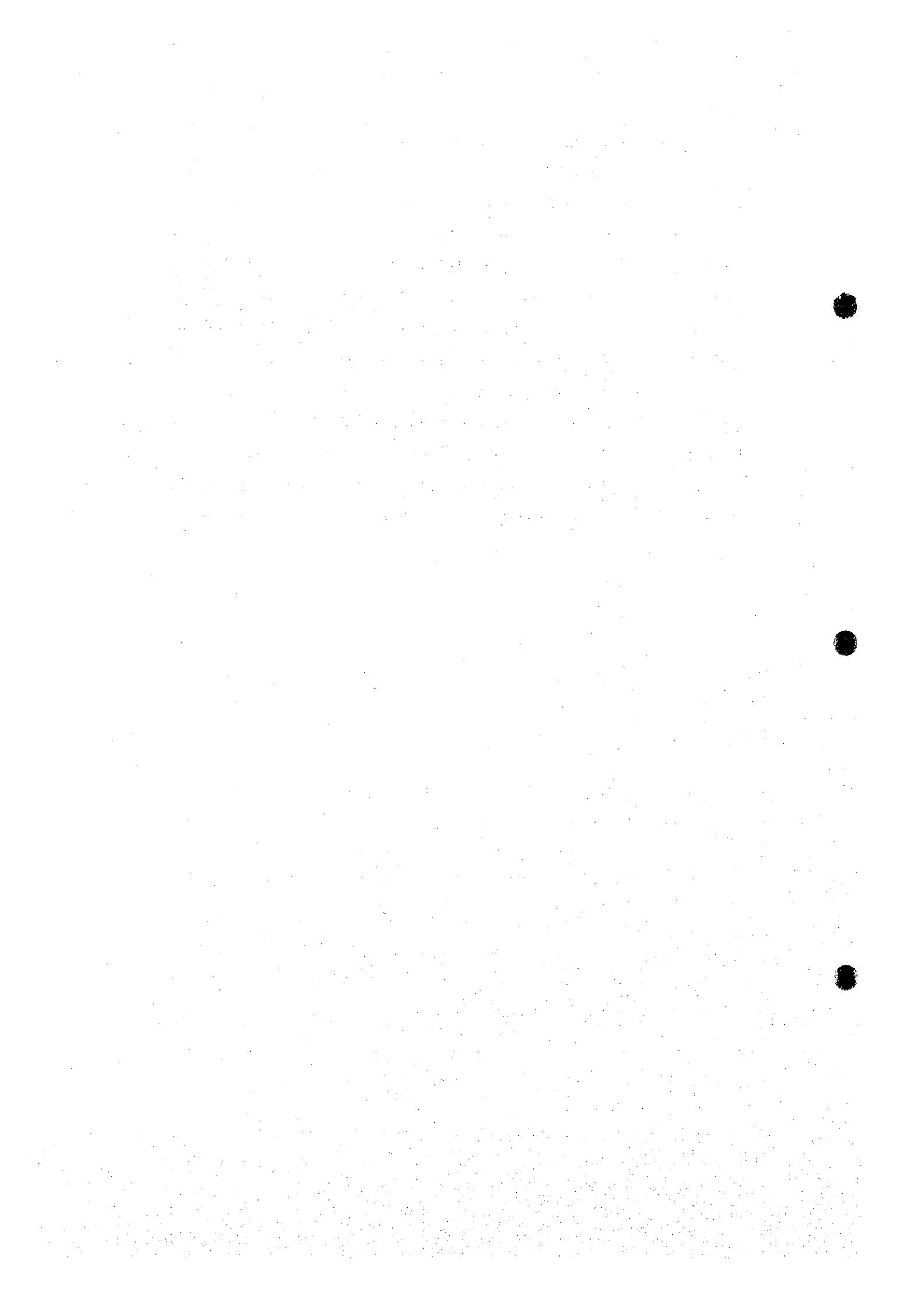
Figure 1-1	Location Map of the Survey Area	2
Figure 2-1-1	Suvey Planning Map	9
Figure 2-4-1	Location Map of Track Line	12
Figure 2-6-1	Location Map of FDC Track Line	14
Figure 2-7-1	Location Map of Baseline Geochemical Survey	15
Figure 2-7-2	Location Map of Sampling Points of Ore Deposit Investigation in the Survey Area	16
Figure 2-9-1	Data Analysis and Processing Flowsheet	17
Figure 2-9-2	Photographs of Survey Equipment and Survey work (1), (2)	19
Figure 3-2-1	Color-coded Bathymetric Map Based on MBES	23
Figure 3-2-2	Bathymetric Map Based on MBES	24
Figure 3-2-3	Bathymetric Profiles	25
Figure 3-3-1	Total Magnetic Force Map	28
Figure 3-3-2	Magnetic Anomaly Map(Trend Surface)	29
Figure 3-3-3	Magnetic Anomaly Map(IGRF)	30
Figure 3-3-4	Magnetic Anomaly Profiles	32
Figure 3-3-5	Reduction to the Pole Anomaly Map	34
Figure 3-3-6	Magnetization Distribution Map	36
Figure 3-3-7	Magnetic Structural Map	40
Figure 3-4-1-1	Geological Structural Map	42
Figure 3-4-2-1	Sound Pressure Images based on MBES	46
Figure 3-4-3	SBP Profile (1), (2)	48
Figure 4-1-1	Location Map of Baseline Geochemical Sampling Points	52
Figure 4-2-1	Schematic Drawings of Sampling Results Obtained from Baseline Geochemical Survey	54
Figure 4-2-2	Species of the Typical Foraminiferal Fossils	59
Figure 4-2-3	Biostratigraphic Zonal Scheme and Events in the Low Latitude Regions	63
Figure 4-2-4	Stratigraphic Distribution of Planktonic Foraminiferal Zones in the studied Cores (1), (2)	64

Figure 4-2-5	Abundance of Each Genus of Planktonic Foraminifera from the studied Cores (1), (2)	70
Figure 4-2-6	Histogram of Grain Size (1)~(3)	76
Figure 4-2-7	Microscopic Photos of Volcanic Sand	84
Figure 5-1-1	Location Map of the Ore Deposit Investigation	94
Figure 5-1-2	Bathymetric Map (94S01 Seamount)	95
Figure 5-1-3	Bathymetric Map (Erromango Basin)	97
Figure 5-1-4	Bathymetric Map (94S02 Seamount)	98
Figure 5-1-5	Bathymetric Map (94S03 Seamount Group)	98
Figure 5-2-1	Seafloor Photographs taken by FDC (1)~(3)	100
Figure 5-2-2	Living Things (1), (2)	103
Figure 5-3-1	Results of Side Scan Sonar Survey (1), (2)	111
Figure 5-4-1	Photos of Sample Collected during Ore Deposit Investigation (1) ~ (3)	117
Figure 5-4-2	Microscopic Photos(Thin Section) (1), (2)	121
Figure 5-4-3	AMF Diagram for Basalts	126
Figure 5-4-4	Diagram using Norm Di-Q-Hy-Ol for Basalts	126
Figure 5-4-5	SiO ₂ versus MgO for Basalts	127
Figure 5-4-6	SiO ₂ versus K ₂ O+Na ₂ O for Basalts	127
Figure 5-4-7	SiO ₂ versus K ₂ O for Basalts	128
Figure 5-4-8	SiO ₂ versus N ₂ O for Basalts	128
Figure 5-4-9	SiO ₂ versus P ₂ O ₅ for Basalts	129
Figure 5-4-10	SiO ₂ versus K ₂ O/TiO ₂ for Basalts	129
Figure 5-4-11	Na ₂ O versus TiO ₂ for Basalts	130
Figure 5-4-12	MgO versus Ni for Basalts	130
Figure 5-4-13	MgO versus Cr for Basalts	131
Figure 5-4-14	MgO versus (Sr/Nd) _n for Basalts	131
Figure 5-4-15	MgO versus (Ba/Ce) _n for Basalts	132
Figure 5-4-16	MgO versus (Rb/La) _n for Basalts	132
Figure 5-4-17	Ce versus Zr for Basalts	133
Figure 5-4-18	(Ce/Yb) _N versus (Ce) _n for Basalts	133
Figure 5-4-19	Zr versus Sr for Basalts	134
Figure 5-4-20	Ba versus Ce for Basalts	134
Figure 5-4-21	Chondrite-normalized Rare Earth Element Patterns for Basalts	135

Figure 5-5-1	Ore Indication Map (1)~(3)	138
Figure 5-5-2	Microscopic Photos of Polished Thin Section (1), (2)	142
Figure 5-5-3	Mn-Fe-(Ni+Co+Cu) × 10 Diagram	148
Figure 5-6-1	Temperature-CTD Depth Profiles (1)~(3)	150
Figure 6-1	Fe-Mn-(Ni+Co+Cu) × 10 Diagram	160

[List of Inserted Tables]

Table 1-1	Survey Apparatus and Equipment	5
Table 1-2	Survey Achievements	6
Table 1-3	Records of Survey Schedule	7
Table 4-2-1	List of Planktonic Foraminiferal Fossils in the Studied Cores ...	6
Table 4-2-2	List of Benthic Foraminiferal Fossils in the Studied Cores	61
Table 4-2-3	Results of Mechanical Analysis of Sediments	79
Table 4-3-3-1	Mean, Standard Deviation, Minimum and Maximum of Chemical Component	92
Table 5-4-1	Results of Chemical Analysis for Rocks	125
Table 5-5-1	Results of Whole Rock Analysis and Trace Level Analysis for Iron-Manganese Oxides (1), (2)	145
Table 5-6-1	List of Temperature Anomalies	149



Chapter 1. Outline of the Survey

1-1 Survey Title

The Fiscal 1994 Joint Basic Study for the Development of Mineral Resources (Study for Marine Resources) in the Exclusive Economic Zone of the Republic of Vanuatu.

1-2 The Purpose of the Survey

The Purpose of the survey is to assess the potential of submarine hydrothermal deposits within the Exclusive Economic Zone of the Republic of Vanuatu, a member of SOPAC, by carrying out a topographical survey, sampling, and other surveys.

1-3 Survey Area

Based on the joint study program on deep-sea mineral resources in the exclusive economic zones of SOPAC member countries as agreed between the Japanese organization assigned for the survey and the South Pacific Applied Geoscience Commission (SOPAC) on March 13, 1990, a polygonal area (of about 37,000km², see Figures 1-1 and 2-1-1) obtained by linking the following coordinates as well as AREA I and a part of AREA II were designated as the survey area. AREA II, however, was excluded from the survey area due to the fact that the area was within the scope of an active area of submarine volcanism and that the depth of water in AREA II was relatively shallow.

AREA I			
No.	Latitude	Longitude	
A	17 ° 35' S	168 ° 44' E	
B	17 ° 11' S	169 ° 41' E	
C	19 ° 56' S	170 ° 58' E	
D	20 ° 20' S	170 ° 00' E	
A	17 ° 35' S	168 ° 44' E	

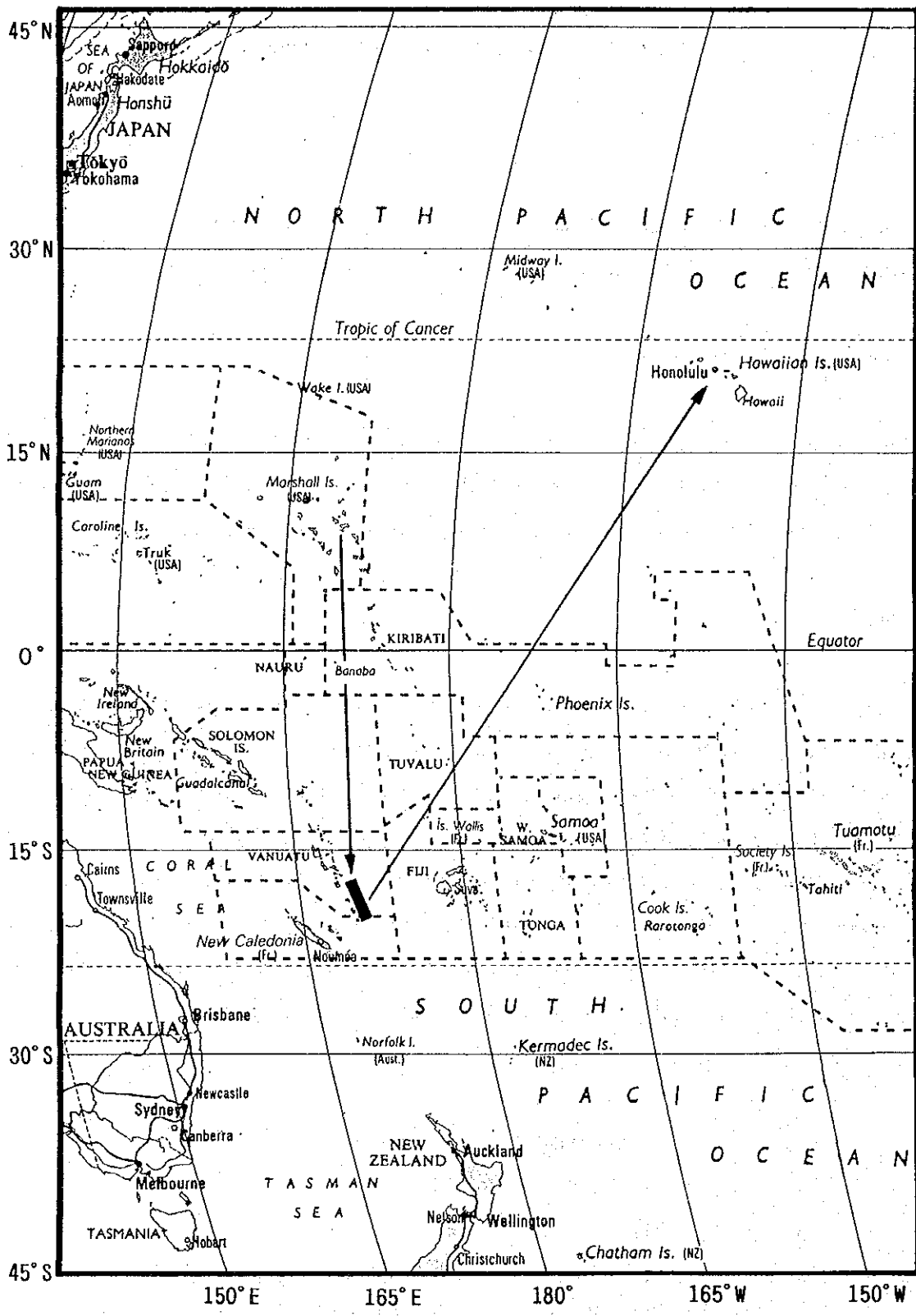


Figure 1-1 Location Map of the Survey Area

AREA II: a part of the area (the environs of Epi Island) within a polygon obtained by linking the following coordinates.

A	17 ° 35' S	168 ° 44' E
B	17 ° 11' S	169 ° 41' E
F	16 ° 14' S	169 ° 04' E
E	16 ° 34' S	168 ° 16' E
A	17 ° 35' S	168 ° 44' E

1-4 Term of the Survey

Survey cruise: August 22, 1994 to October 25, 1994 (66 days)

Analysis and others: April 1, 1994 to March 31, 1995

1-5 Survey Participants

Japanese Participants

Field Supervisors

Koji HIRAI (Metal Mining Agency of Japan)(from Sept. 20 to October 25)

Kokichi IIZASA (Geological Survey of Japan, Agency of Industrial Science and Technology)(from Sept. 20 to October 25)

Members:

Leader	Kiyoshi KAWASAKI (DORD: Deep Ocean Resources Development Co., Ltd.)
Chief Geologist	Taizo MATSUMOTO (DORD)
Geologist	Nobuyuki OKAMOTO (DORD)
Geologist	Hikaru SORAOKA (DORD)
Geologist	Masahiro NARA (DORD)
Geologist	Tadayuki ISHIYAMA (DORD)
Geologist	Yosuke SAKAGAMI (DORD)
Geologist	Yutaka HASHIMOTO (OED: Ocean Engineering and Development Co., Ltd.)
Chief Geophysicist	Kohei MAEDA (DORD)
Geophysicist	Nadao SAITO (DORD)
Geophysicist	Osamu DEGUCHI (DORD)

Geophysicist	Seigo UESAKA	(DORD)
Geophysicist	Kazuhiko KASHIWASE	(DORD)
Geophysicist	Masakatsu OGURO	(DORD)
Geophysicist	Takatsugu SHIBAHASHI	(DORD)
Geophysicist	Keisuke MATSUMURA	(DORD)
Geophysicist	Tadashi SATO	(OED)
Geophysicist	Takeharu AISAKA	(OED)

Consigning Participants

Trainees

Mr. Victor Rory (Vanuatu)(from Aug. 20 to Sept. 20)

Mr. Makali Arsen (Vanuatu)(from Sept. 20 to Oct. 25)

1-6 Survey Apparatus and Equipment

Major apparatus and equipment used during the survey are listed in Table 1-1.

1-7 Survey Achievements

Survey operations were accomplished as shown in Table 1-2 and Table 1-3.

Table 1-1 Survey Apparatus and Equipment

	Survey Method	Survey Apparatus and System	Abbreviation	Remarks
Positioning	Satellite Navigation	Global Positioning System	GPS	
Sea Bottom Topo-	Acoustic Sounding Bathymetry	Multi-narrow Beam Echo Sounder	MBBS	
		Narrow Beam Echo Sounder	NBS	
	Subsurface Geological Structure	narrow-Sub Bottom Profiler Side Scan Sonar	nSBP SSS	
	Magnetic Survey	Proton Gradio Meter	PGM	
	Seawater Survey	Conductivity, Temperature and Pressure Measuring System	CTD TD	
	Sampling	Large Gravity Corer Gravity Corer Chain Bucket Finder Mounted Power Grab	LC GC CB FPG	
Sea Bottom Observation	Photograph and TV	Continuous Deep Sea Camera with Finder	FDC	with CTD
	Photograph	Deep Sea Camera		with LC, GC
Data Recording and Processing	On-Line Functions Data Strirage Functions Off-line Functions ↓ Track Line Maps Various Plan Maps Cross Sections Date Analysis	Data Processing System Sensor CPU File Sever CPU Host CPU Engineering Work Station (EWS) Local Areal Network(LAN) Personal Computer(PC) Intelligent Color Monitor (ICM)	DPS	

Table 1-2 Survey Achievements

	Item	Accomplishment
Survey Schedule	Depart Majuro Start the Survey Finish the Survey Arrive Port-Vira Depart Port-Vira Start the Survey Finish the Survey Arrive Honolulu	Aug. 22 16:00 Aug. 27 17:40 Aug. 18 16:04 Sep. 19 08:00 Sep. 22 16:00 Sep. 23 07:30 Oct. 14 24:00 Oct. 25 08:00
Sampling	baseline Geochemical Sampling	17 points (GC 10 times, LC 7 times)
	Ore Deposits Survey	31 points (LC 21 times, FPG 8 times, CB 2 times)
	Weight of Taken Samples	Hydrothermal Precipitates 629.0kg Rocks 472.5kg Muddy Sediments 1,248.0kg Total 2,349.5kg
Deep Sea Observation (FDC)	Number of Track lines Total Length of the Lines Acquired Photographs	7 Track lines 61.9 nautical miles 2,560 sheets No. 1 line 350 sheets 7.5miles No. 2 line 92 sheets 4.3miles No. 3 line 71 sheets 2.4miles No. 4 line 159 sheets 3.6miles No. 5 line 154 sheets 2.4miles No. 6 line 114 sheets 3.6miles No. 7 line 45 sheets 1.6miles No. 8 line 186 sheets 7.4miles No. 9 line 171 sheets 7.3miles No. 10 line 176 sheets 2.5miles No. 11 line 220 sheets 2.5miles No. 12 line 235 sheets 2.2miles No. 13 line 167 sheets 2.5miles No. 14 line 120 sheets 3.4miles No. 15 line 172 sheets 4.0miles No. 16 line 84 sheets 3.1miles No. 17 line 41 sheets 1.6miles
Physical Property Survey	CTD (Vertical Type) (Towed Type) Magnetic Survey (PGM)	2 pints 17 lines (with FDC) 5,528.9 miles
Acoustic Sound- ing	MBES (15.5khz)	6,690.3 miles
	NBS (30.0khz)	ditto
	nSBP (3.5khz) SSS (59.5khz)	ditto 12.4 miles (3 lines)
Data Processing	MT from Data Processing System (No. 5 Labo.) MT from MBES Drawing	1 reel (Off-Line) 25 reels (On-Line)

Date and Time are shown in the Local Time.

Table 1-3 Records of Survey Schedule

Month/Day		Survey Items	Month/Day	Survey Items
01	08/22	Mo	32	Th
02	08/23	Tu	33	Fr
03	08/24	We	34	Sa
04	08/25	Th	35	Su
05	08/26	Fr	36	Mo
06	08/27	Sa	37	Tu
07	08/28	Su	38	We
08	08/29	Mo	39	Th
09	08/30	Tu	40	Fr
10	08/31	We	41	Sa
11	09/01	Th	42	Su
12	09/02	Fr	43	Mo
13	09/03	Sa	44	Tu
14	09/04	Su	45	We
15	09/05	Mo	46	Th
16	09/06	Tu	47	Fr
17	09/07	We	48	Sa
18	09/08	Th	49	Su
19	09/09	Fr	50	Mo
20	09/10	Sa	51	Tu
21	09/11	Su	52	We
22	09/12	Mo	53	Th
23	09/13	Tu	54	Fr
24	09/14	We	55	Sa
25	09/15	Th	56	Su
26	09/16	Fr	57	Mo
27	09/17	Sa	58	Tu
28	09/18	Su	59	We
29	09/19	Mo	60	Th
30	09/20	Tu	61	Fr
31	09/21	We	62	Sa
			63	Su
			64	Mo
			65	Tu

Chapter 2. Survey Methods

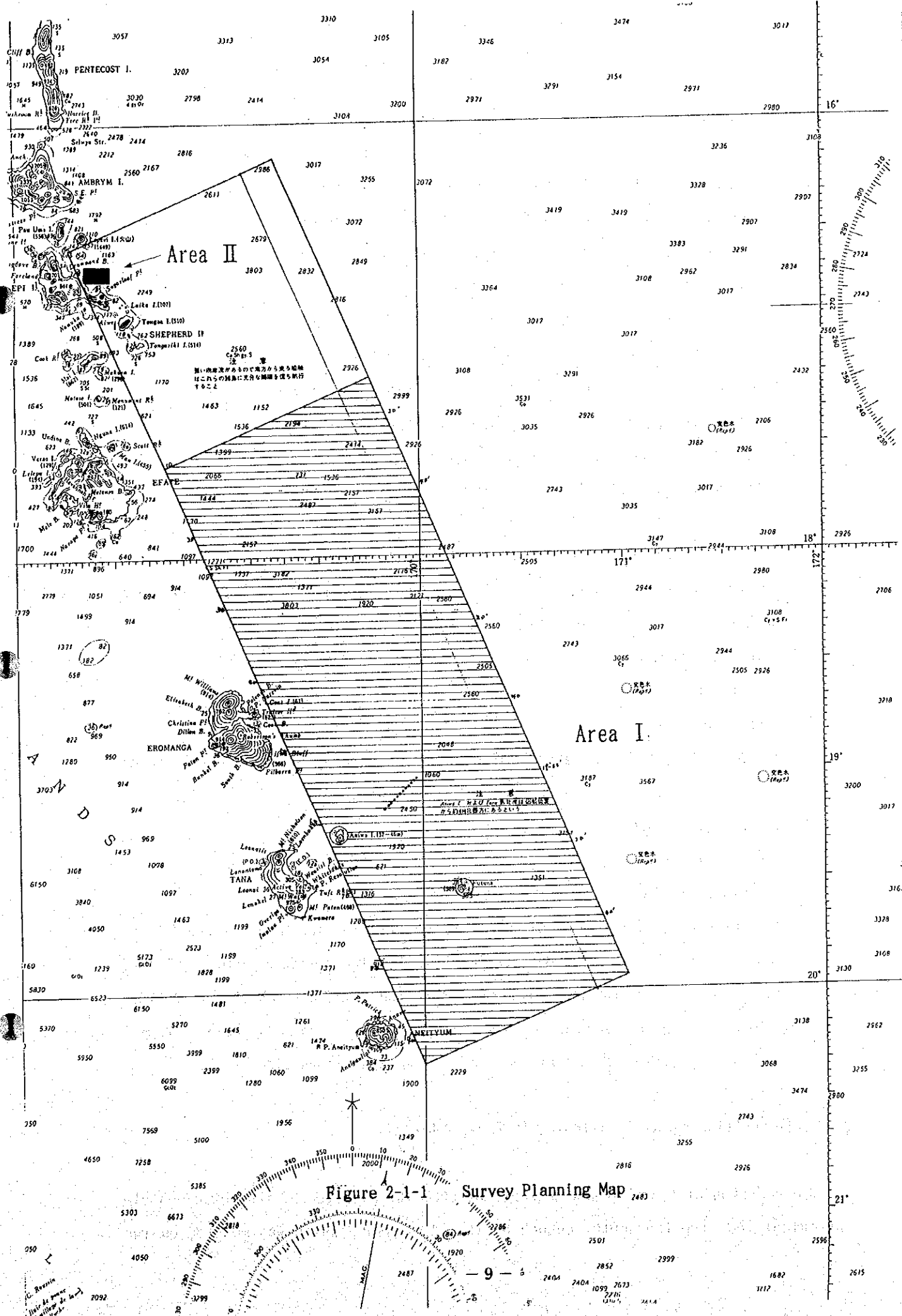
2-1 Survey Procedures

In 1994, the fifth fiscal year of the Second Phase of the five year SOPAC Program, a topographical survey and a survey related to submarine hydrothermal deposits were carried out, as planned, within the exclusive economic zone of the Republic of Vanuatu (see Fig. 2-1-1).

A regional survey was carried out in the survey area during the first half of the schedule (LEG 1). The regional survey was composed of topographical and magnetic surveys and baseline geochemical samplings at intervals of 2 miles. During the second half of the schedule (LEG 2), areas for carrying out the ore deposit investigation were selected on the basis of the results obtained from the topographical and magnetic surveys. Deep-sea observation by FDC, SSS surveys and sampling were carried out in the selected areas.

Principal work for the survey was comprised of the following;

- (1) Topographical surveys were carried out at a speed of 10 knots by employing GPS and MBES so as to identify accurate geographical features. Additional interpolation track-lines at intervals of 1 mile were established in areas where the depth of water was relatively shallow.
- (2) In order to estimate the geological structure, magnetic surveys were carried out in parallel with the topographical surveys.
- (3) Samples for the baseline geochemical survey were collected from the southern part of the survey area (in the neighborhood of 19° 04' S, 169° 55' E) on an approximately 1-mile grid (13 sampling points) by employing GC or LC.
- (4) Deep-sea observation by FDC was carried out at 17 track lines totaling 61.9 miles.
- (5) SSS surveys were carried out at mineralized zones and alteration zones, which had been observed by FDC, at 3 track lines totaling 12.4 miles.
- (6) Sampling operations were carried out at the mineralized and alteration zones.



2-2 Numbering

Sampling points and track lines were numbered in the following manner;

- For the sampling points of the baseline geochemical survey:

Year-S-B-Equipment employed (two letters) - No..

Examples: 94SBLC01 (when LC was used)

: 94SBGC01 (when GC was used)

In these cases, "S" indicates "SOPAC," "B" indicates

"Baseline" and "No." indicates the serial number starting from 01.

- For the sampling points of the ore deposit investigation:

Year-S-D-Equipment employed (two letters) - No.

Examples: 94SDPG01 (when FPG was used)

94SDL01 (when LC was used)

94SDCB01 (when CB was used)

In these cases, "S" indicates "SOPAC," "D" indicates "(Ore) Deposit" and

"No." indicates the serial number starting from 01.

- For the FDC track lines:

Year-S-FDC-No.

Example: 94SFDC01

In this case, "S" indicates "SOPAC" and "No." indicates the serial number starting from 01.

- For the acoustic sounding track lines:

No. - Division - 0 ~ 9

Example: 16-0-0

In this case, "No." indicates the serial number of the main track line numbered at intervals of 2.0 miles counting from the northern side, "Division" indicates the division number of the track line (when a track line is divided into several portions) and the serial number starts from zero. Figures from 0 to 9 at the last section indicate the interpolation track lines.

2-3 Ship Positioning and Positioning of Towed Vehicle

The position of the ship was measured by GPS. The position of the towed vehicle was calculated from the depth sounded by the CTD Sensor, which was mounted on the

towed vehicle, and the length of the cable by applying the Pythagorean formula.

As for the system of geodetic coordinate, WGS84 was used. And 165° E Local time (GMT+ 11 hours) was used for the inboard time.

2-4 Acoustic Sounding

Submarine topographic surveys covering the entire survey area were carried out by establishing track lines at intervals of 2.0 miles, but an interpolation track line was added between two main track lines where the depth was relatively shallow.

Furthermore, areas with a depth of less than 500m and areas within 3.0 miles from land were excluded from the survey area (see Fig. 2-4-1).

Bathymetry readings were made at every 5 ~ 10 seconds for MBES and every 8 seconds for NBS while the ship was cruising at speeds of about 10 knots.

2-5 Magnetic Survey (PGM Survey)

A magnetic survey was made simultaneously with the submarine topographic survey in the hope that the magnetic survey would help us to elucidate the geological structure of the survey area. The collection of data, however, was made only at the main track lines through the topographic survey.

In order to protect the PGM Sensor from interference of magnetism existing within the ship, the PGM Sensor was towed by a cable from the stern. The distance from the stern to the sensor was set at 710m. The total magnetic intensity was measured by the sensor every 6 seconds at the sensitivity of 0.1 gamma.

Measured data was on-line recorded in the DPS every 10 seconds before the data was processed.

2-6 Seafloor Observation and Photography

Real-time sea-floor observation was made through color images by towing FDC, on which a still camera, a TV camera and CTD were loaded, around selected waters including ridges in troughs as well as sea-mounts, at cruising speeds of about 1 knot, and taking colour photographs at places having characteristic features.

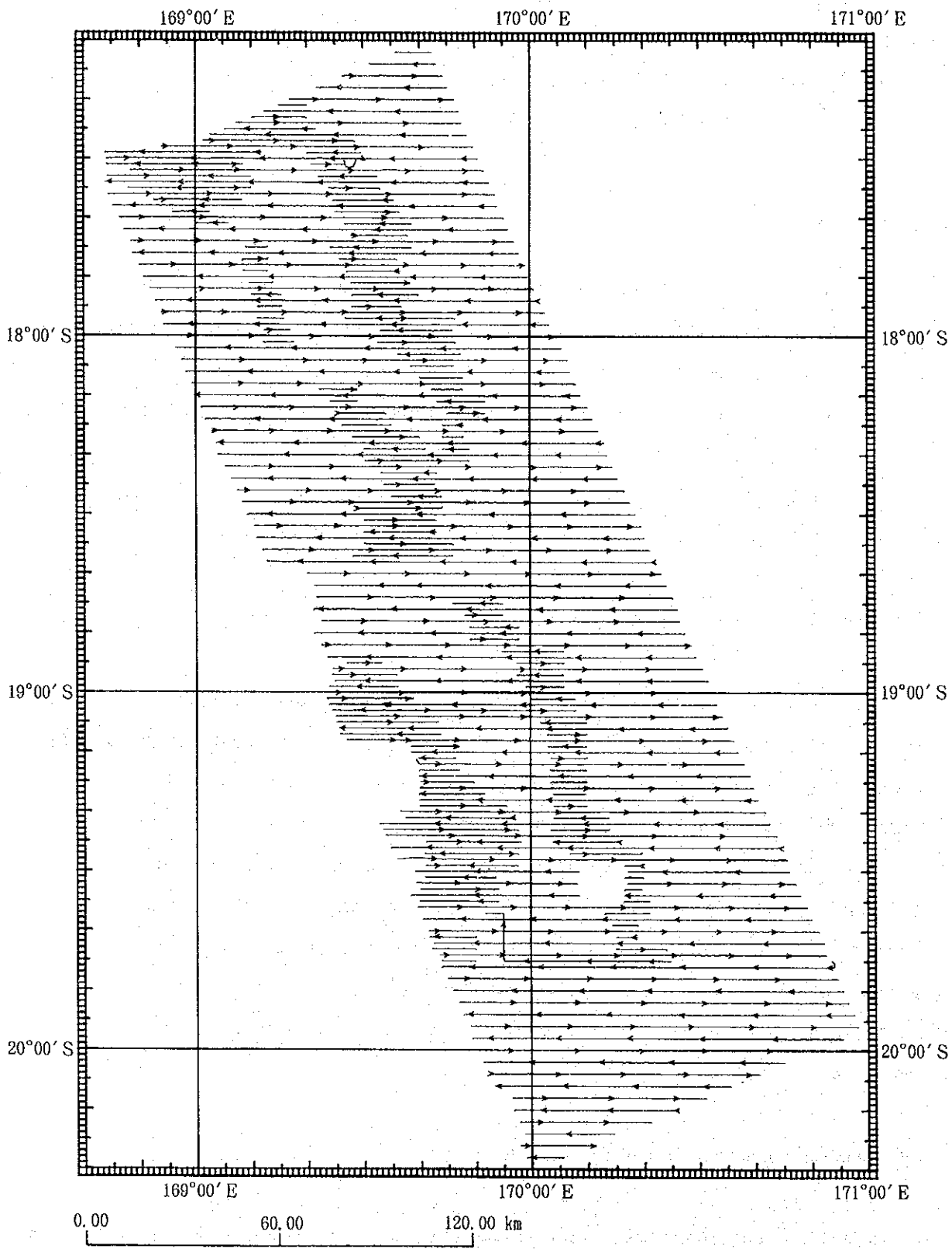


Figure 2-4-1 Location Map of Track Line

The resulting seafloor images were recorded on videotape.

The length of track lines was set at 1.6 ~ 7.5 miles. The towing direction was mainly set to N → S ~ NW → SE by considering the direction of the wind and tides (see Fig. 2-6-1).

2-7 Sampling

A baseline geochemical sampling was made at 13 points at intervals of 1 mile by setting a track line of about 12 miles (see Fig. 2-7-1). GC or LC was used about four times per day for sampling. There were, however, some cases in which samples were not collectable. In such cases, additional operations were tried at the same points. By doing so, some samples were collected from certain points. In such cases, only the results of the second operation were indicated on the maps and in the tables showing the results of the baseline geochemical sampling (Chapter 4 and Table 1 to Appendix).

Sampling for the ore deposit investigation was carried out at places where alteration zones had been identified in advance by the FDC survey.

LC, FPG and CB were appropriately selected and employed to collect samples for the ore deposit investigation (see Fig. 2-7-2).

2-8 Survey on Sea Water (CTD Measurement)

In order to obtain values of depth versus sound velocity for MBES, a vertical CTD survey was carried out at two measuring points.

In order to identify signs of hydrothermal activity, data on water temperature, salinity, water pressure and others were collected every 5 seconds by FDC-mounted CTD for analysis.

Furthermore, the depth of water which was calculated from FDC-mounted CTD was used to calculate the location of the towed vehicle.

2-9 Processing and Analysis of Survey Data

The data was processed and analyzed by DPS and a personal computer as shown in the Data Processing and Analysis Flowsheet (Fig. 2-9-1). Basic data was processed and analyzed on board, and a cruise report was written.

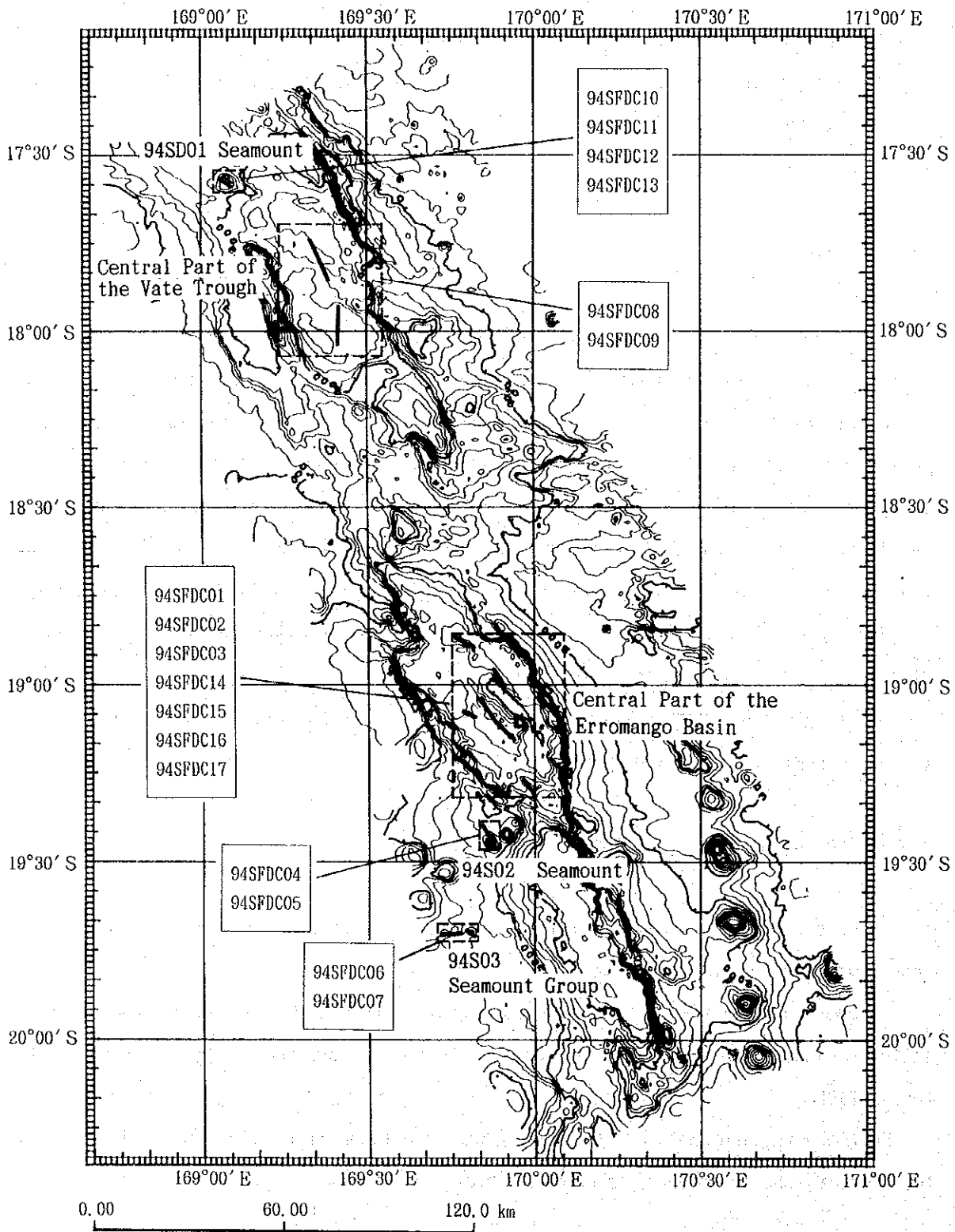


Figure 2-6-1 Location Map of FDC Track Line

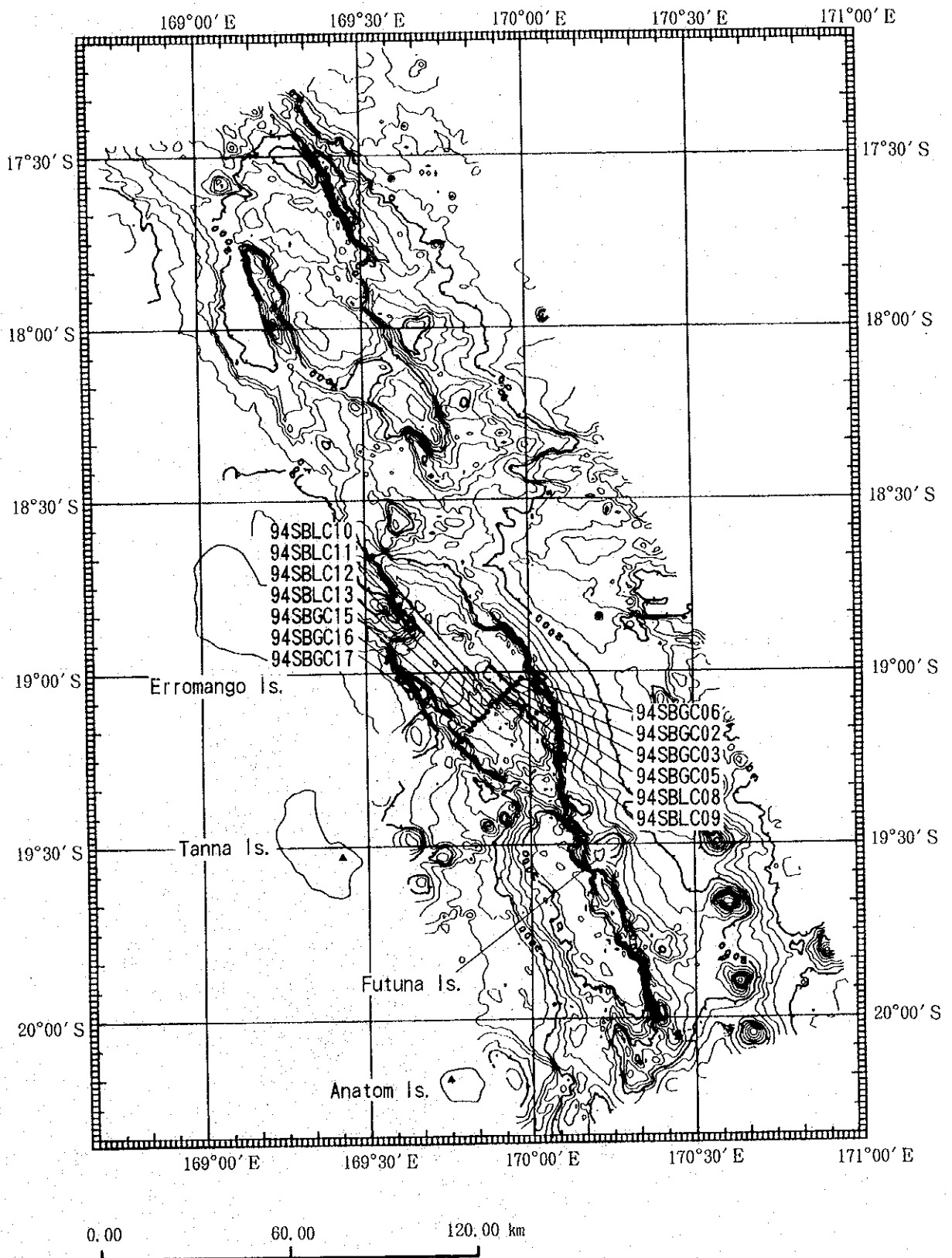


Figure 2-7-1 Location Map of Baseline Geochemical Survey

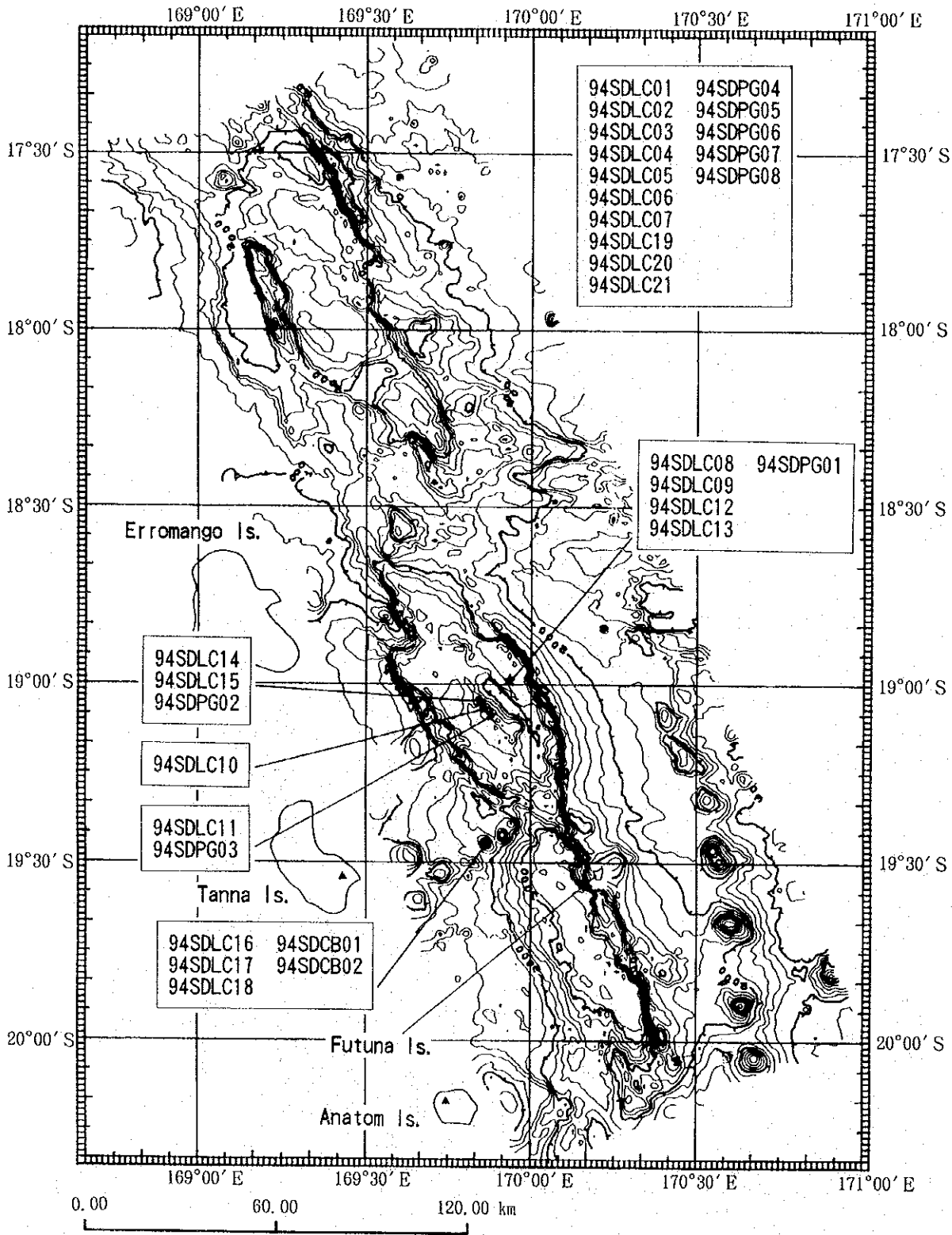
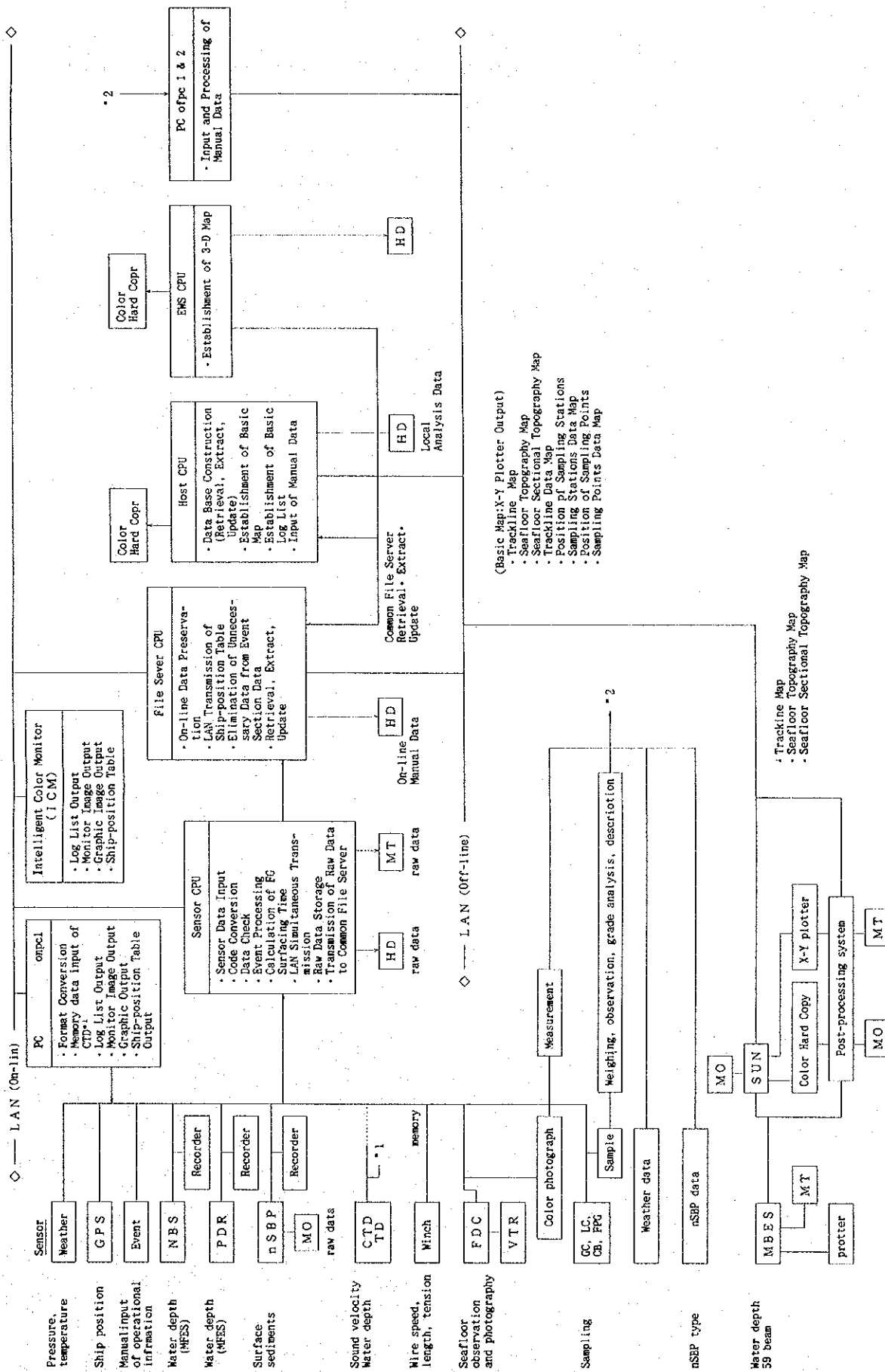


Figure 2-7-2 Location Map of Sampling Points of Ore Deposit Investigation in the Survey Area



(Basic Map: X-Y Plotter Output)

- Trackline Map
- Seafloor Topography Map
- Seafloor Sectional Topography Map
- Trackline Data Map
- Position of Sampling Stations
- Sampling Stations Data Map
- Position of Sampling Points
- Sampling Points Data Map

- Trackline Map
- Seafloor Topography Map
- Seafloor Sectional Topography Map

Figure 2-9-1 Data Analysis and Processing Flowsheet

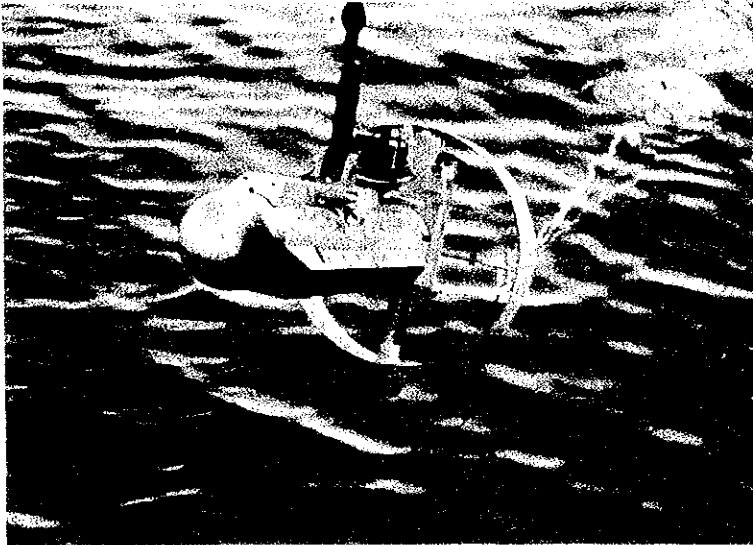
Various tests, studies and analyses were made on shore afterward and the present report was produced by combining both results.

Grade analysis and X-ray diffraction were conducted on manganese oxides and other substances obtained by sampling operations to determine their mineral composition.

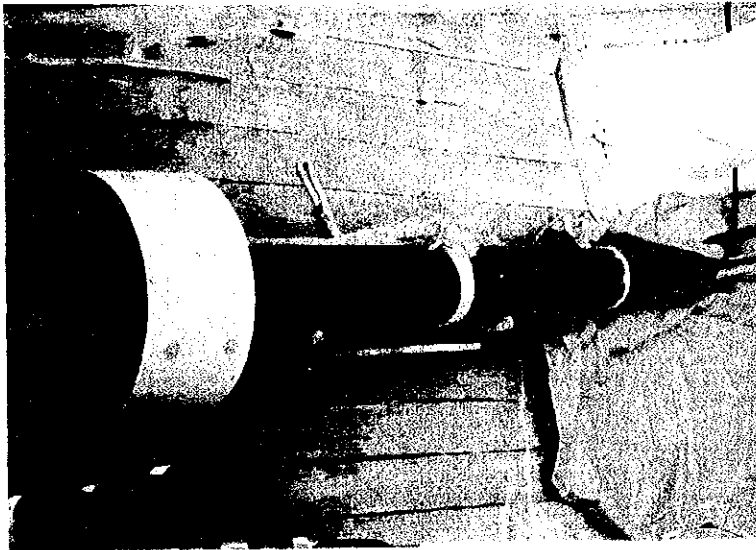
Chemical analysis and microscopic observation were performed on rock samples to determine their mineral composition and texture.

Chemical analysis, X-ray diffraction, size distribution measurement and microfossil identification were carried out on sediments.

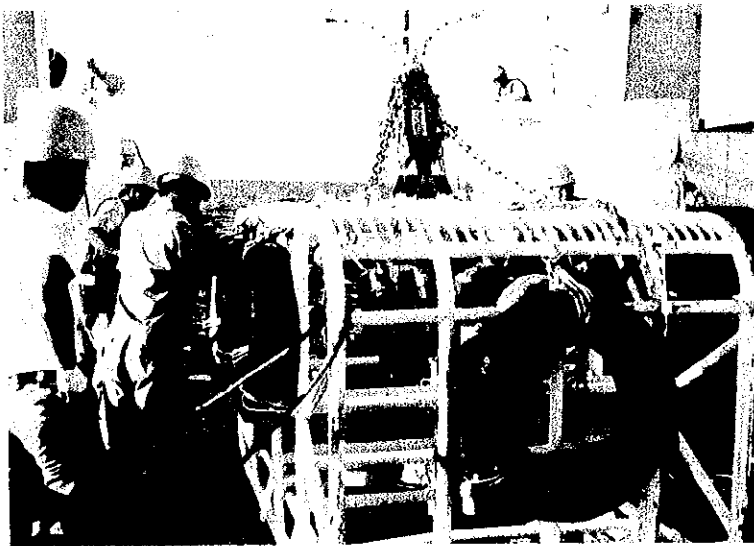
Figures 2-9-2 (1) and (2) show the types of apparatus and equipment employed for the survey and how they were used.



Side Scan Sonar



Proton Gradio Mater

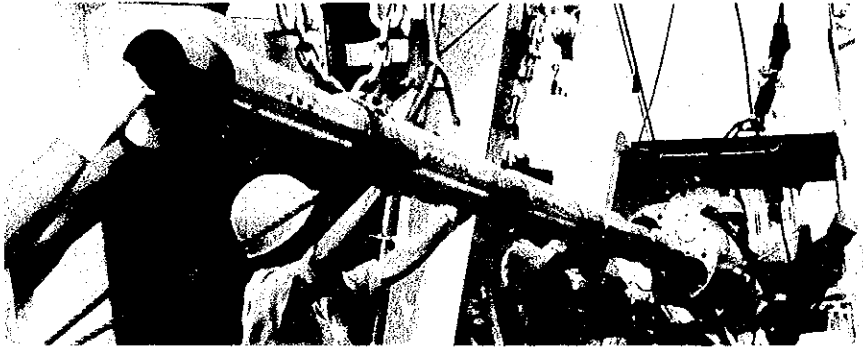


Continuous Deep Sea
Camera with Finder

Figure 2-9-2 Photographs of Survey Equipment and Survey work (1)



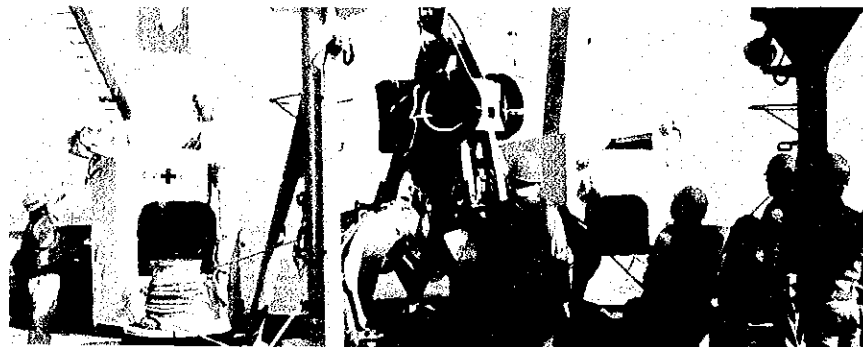
Gravity Corer



Large Corer



Chain Bucket



Finder mounted Power Grab

Figure 2-9-2 Photographs of Survey Equipment and Survey work (2)

Chapter 3. Seafloor Topography and Geological Structure

The Republic of Vanuatu is a portion of the New Hebrides Arc, located at the point where the archipelago extending to Papua New Guinea and the Solomon Islands bends to south. The New Hebrides Arc is situated in the south and extends to the Fiji and Tonga island arc in the east beyond the Hunter Fracture Zone. This is where the Pacific Plate to the north and east and the India-Australia Plate to the west and south collide. The New Hebrides Arc is adjacent to the North Fiji Basin, opened up by the collision, on the east side, and on the west side it is adjacent to the New Hebrides Trench which was formed through subduction of the India-Australia Plate.

3-1 Outline of the Survey Area

The survey area is located to the east of Efate, Erromango, Tanna and Anatom Islands. These islands are roughly located in the NNW ~ SSE direction of the exclusive economic zone of the Republic of Vanuatu, which is located to the west of the North Fiji Basin. The survey area covers the entire waters of the Coriolis Troughs that develops in this area.

The Central Chain, a volcano of the New Hebrides Trench, stretches in the direction of NNW ~ SSE for about 1,200km from the north (Santa Cruz) to the south (Anatom) on the west of the survey area.

Existence of a number of submarine volcanoes in and around the survey area is known and the potential for the origin of hydrothermal deposits were pointed out by scholars (Cronan, 1981). Also, according to reports by Crawford et al, there are a number of calderas between Epi Island and Efate Island in addition to four submarine volcanoes (Epi a, b, c and Karua) that have been active since the Pliocene, and potentialities of the existence of hydrothermal ore deposits are pointed out. Furthermore, according to Recy et al, volcanic activity in this area is concomitant with upheaval of the marginal sea in the early part of its spreading and the potential for the generation of hydrothermal deposits is high.

According to recent report (C. Robin et M. Monzier, 1994), the history of violent volcanic activity in Vanuatu is rather new and, tracing back less than 2,000 years.

It was reported that the area of the archipelago from Ambrym to Efate Islands is still the site of the most significant volcanic activity. The Coriolis Troughs elongate, rhomboidal depressions with steep walls and flat floors, formed by extension. This trough is composed of three distinct structures, namely the Vate Trough, Erromango Basin and Futuna Trough forming a line from north to south. The Futuna Trough is relatively immature and like Erromango Basin, shows no recent volcanism. The Vate Trough is the most developed, and its floor is largely covered by lava fields (R. C. Price, P. Maillet, D. P. Johnson, 1993).

3-2 Submarine Topography

A colour-coded bathymetric-contour map and bathymetric map of the survey area are shown in Figures 3-2-1 and 3-2-2. A typical bathymetric profile is shown in Fig. 3-2-3. As stated above, the survey area is the SE slope of the New Hebrides Arc. The Coriolis Troughs which is considered to be a back arc basin, is located at the central part of the survey area.

The Coriolis Troughs forms a concave area, about 40km wide and about 2,600m deep (maximum depth of about 3,400m), with its major axis of about 320km lying in the NNW-SSE direction. Cliffs on both east and west sides of the trough are steep, and represent a relative height of about 1,000m on the whole, while the eastern cliff is greater in cliff-top depth, relative height and inclination. The northern tip of the trough is outside of the survey area, and therefore is undefined. The arc slope faces south at the southern end of the survey area, where the the major part of the Coriolis Troughs ends. Therefore, the lower portion of the North Fiji Basin shows the tendency to approach to the western trench.

Due to the presence of sill around 18° 30'S and 19° 20'S points, the inner part of the Coriolis Troughs is further divided into three basins, named, from north to south, the Vate Trough, the Erromango Basin and the Futuna Trough.

The east and west sides of the Trough represent a arc platform of the New Hebrides Arc. The west side gets shallower toward the center of the arc, while the east side deepens gradually toward the North Fiji Basin floor. A group of knolls of the relative height of about 300m are observed on the northern side of the survey area and seamounts chain of the relative height of about 1,000m are seen on the southern side, in the area close to the place where the North Fiji Basin floor and the arc

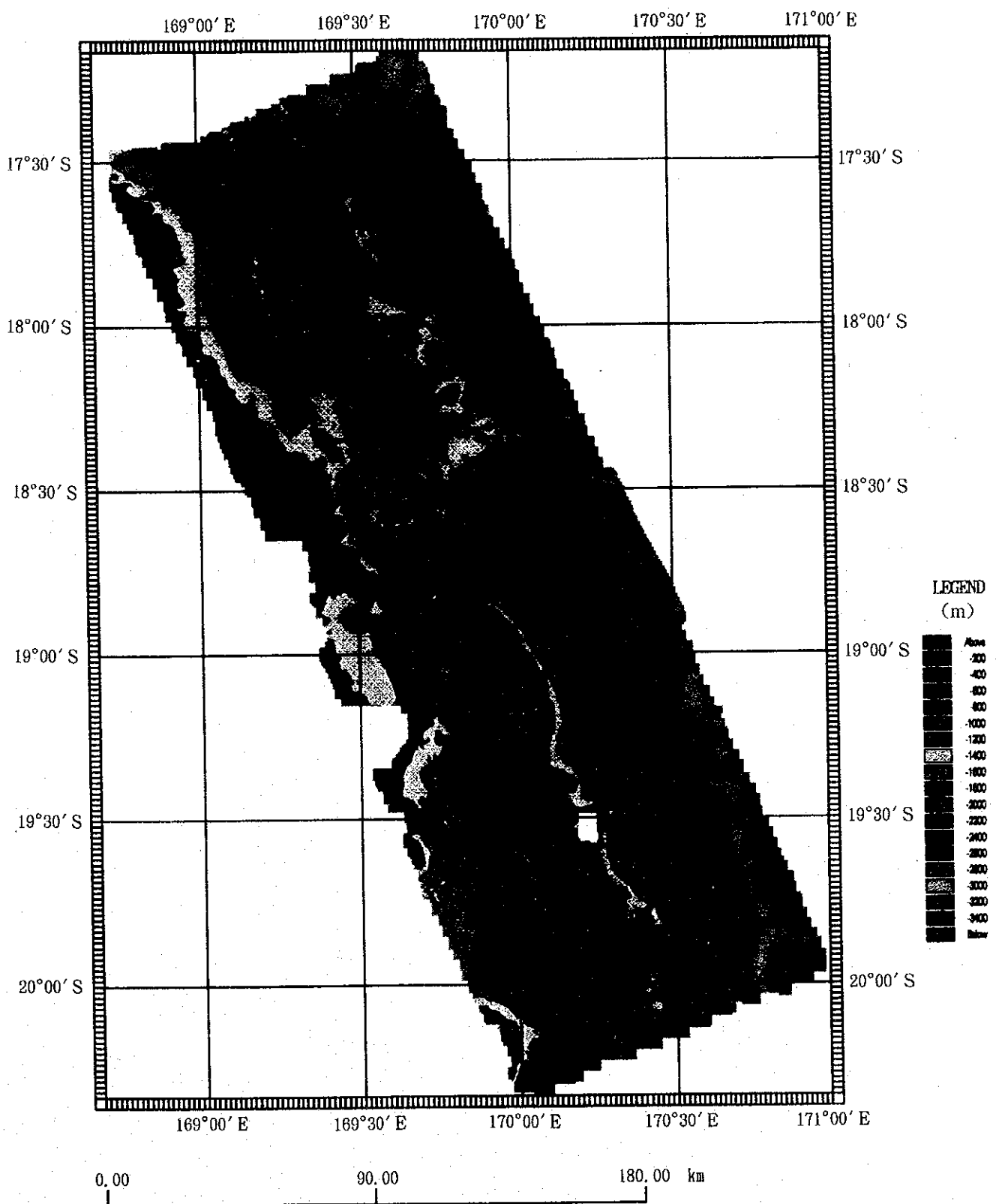


Figure 3-2-1 Color-coded bathymetric map based on MBES.
Color change and contour interval is every 200m

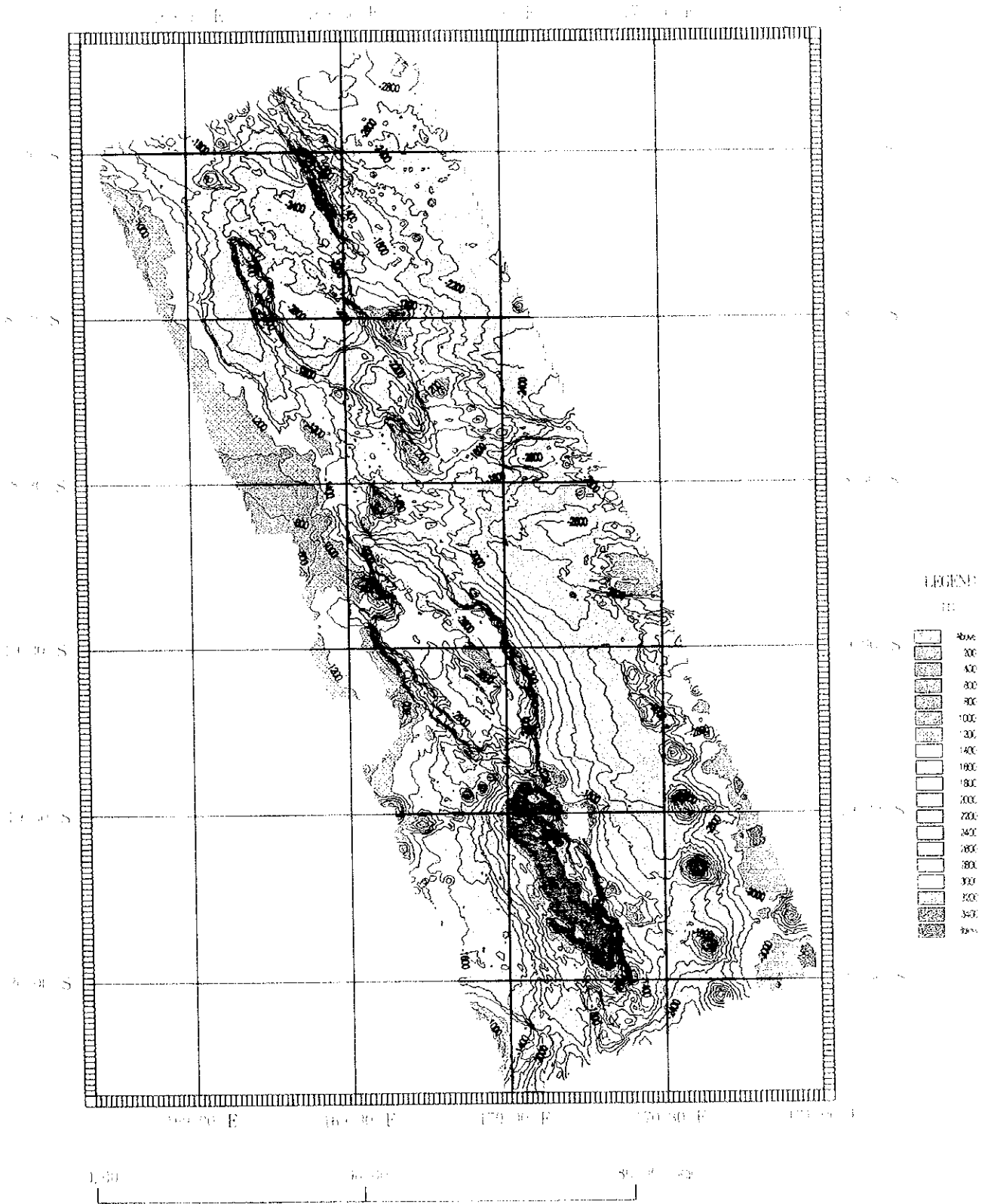
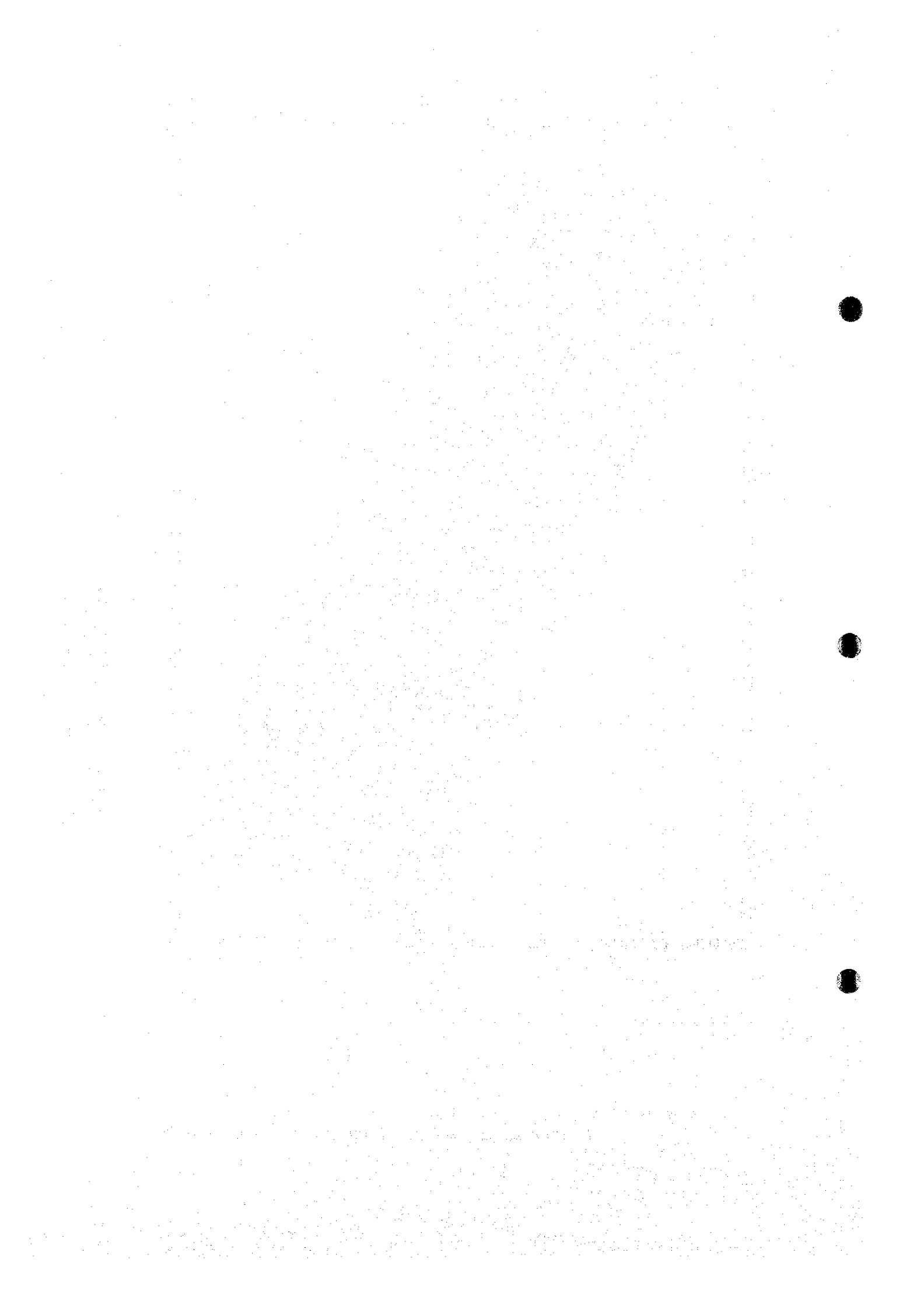


Figure 3-2-1 Color coded bathymetric map based on MBES. Color change and contour interval is every 200m



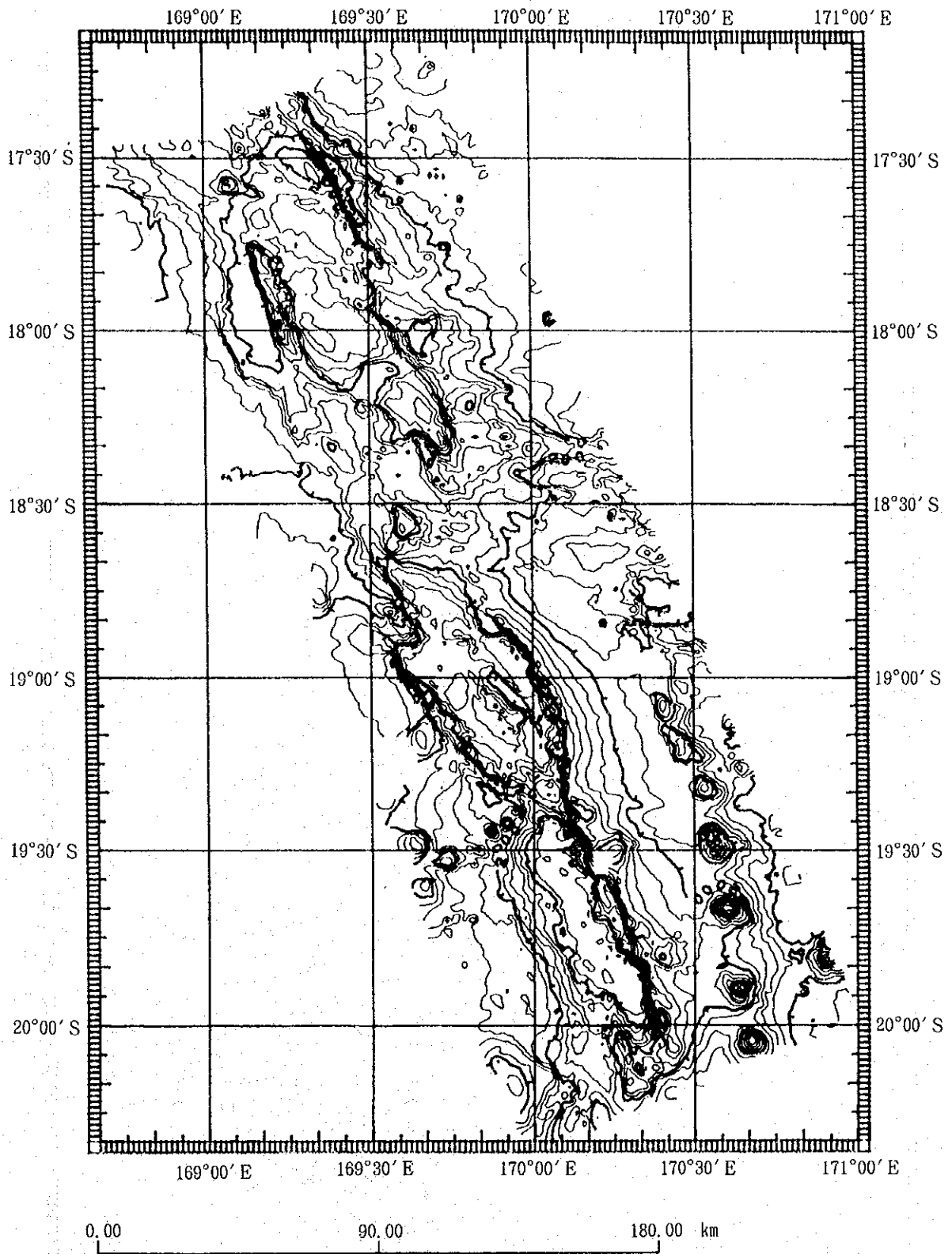


Figure 3-2-2 Bathymetric map based on MBES.
 MBES data are gridded at an about 1.5-km spacing.
 Contour interval is 200m

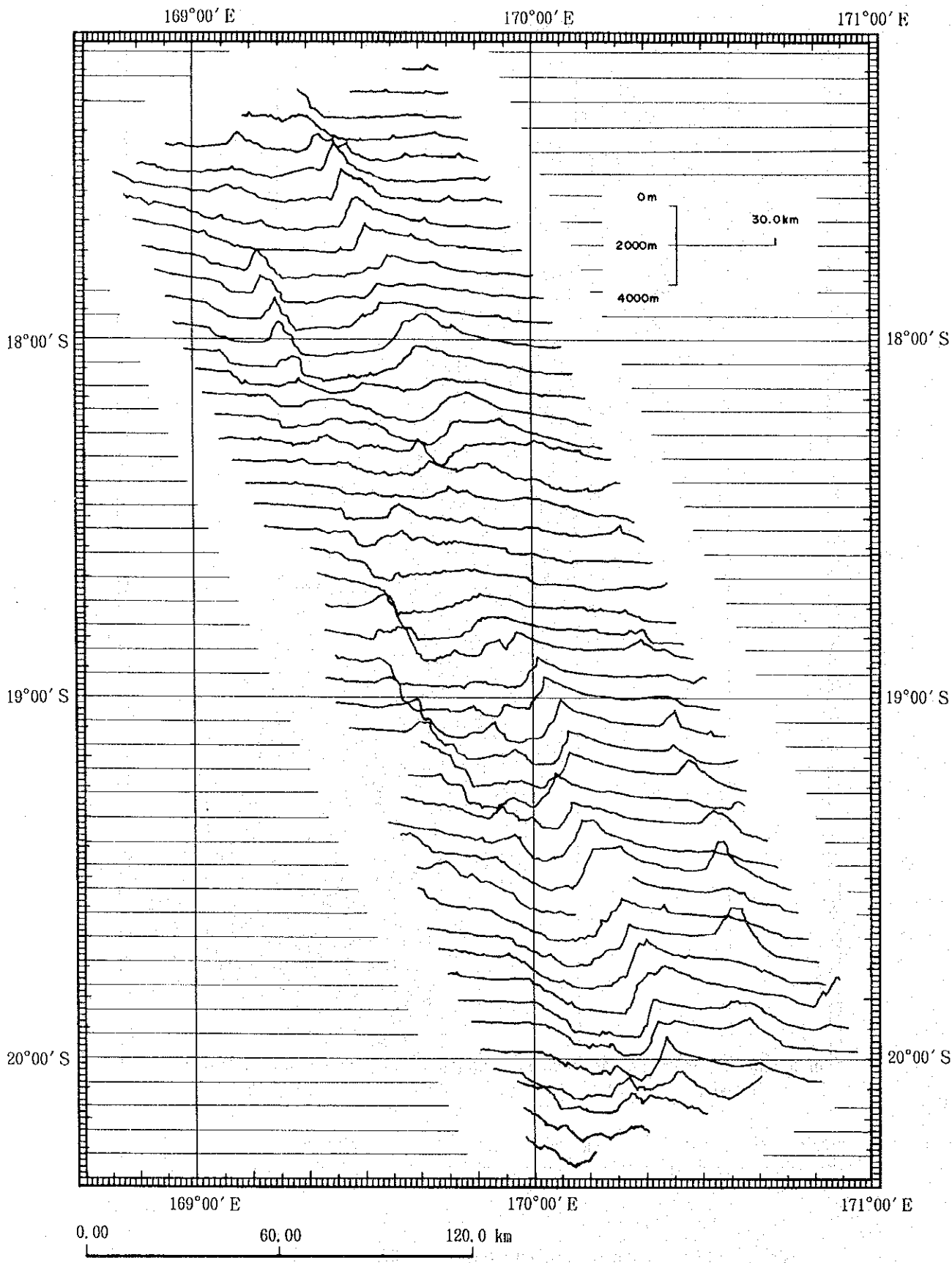


Figure 3-2-3 Bathymetric Profiles

slope meet.

Each of the Troughs is further described as below:

(1) Vate Trough

The Vate Trough is located in the north part of the Colioris Troughs, which is in the east of the Efate Island. It forms a basin of about 60km wide and about 120km long to the NNW-SSW direction. The bottom of the Trough is approx. 2,500m deep. Both the east and west sides of the Trough connecting to the arc slope form a steep cliff, the relative height being about 400m on the west and about 1,200m on the east.

Around the center of the Vate Trough, 17° 55'S - 169° 13'E, is a ridge, 10km wide and 35km long, in parallel to the extension of the Trough. The shallowest part of the ridge is about 1,000m in depth. The Trough is divided into three basins: one in the north, one in the east and one in the west. The north of the ridge forms a basin about 2,500m deep to the WNW-ESE, intersecting diagonally with the axis of the Trough. In the east of the ridge, a depression (about 2,800m deep) around 18° 00'S-169° 20'E continues to another depression in the southeast (about 2,500m in depth) with a plateau (about 1,800m in depth) in-between. Each of these deeps forms a trough about 30km wide and 80-90km long. Unlike these basins in the north and in the east, the depression in the west of the ridge is of a smaller scale, 15km wide, 60km long and 2,100m in depth.

The area around 18° 20' - 35'S exhibits a rise of 600 to 1,100m deep, forming a treshhold between the Vate Trough and the Erromango Basin in the south. A small basin, about 1,700m deep, is observed on the rise.

(2) Erromango Basin

The Erromango Basin, located to the east of Erromango Island and Tanna Island, is a trough, with major axis of about 120km long to the NNW-SSE direction, a minor axis about 50km and a depth about 2,700m. The slope from the arc platform to the Basin exhibits a steep cliff, similar to the Vate Trough, showing a relative height of about 1,200m in the west and about 1,600m in the east. A ridge-shape configuration is seen to the NW-SE on both north and south sides between the deepest part (3,600m) of the Basin. The northern ridge is 2,400m in depth at its summit, while the southern one (center ridge) is 2,100m. There is another rise,

about 2,300m deep at its top, further south on the southern ridge with a depression in-between. This rise also exhibits a ridge (south ridge).

(3) Futuna Trough

The Futuna Trough is distinguished from the Erromango Basin by a threshold about 2,000m deep around 19° 20' S. This is a trough whose major axis extends about 80km to the NNW-SSE direction while the minor axis is about 35km. It is 3,100m deep (maximum depth of about 3,400m), and is the deepest trough of the three. The shoulder part of the slope from the arc platform to the trough bottom is about 1,800m deep in the west and 1,400-1,500 deep in the east. It is therefore shallow in the east and deep in the west.

3-3 Magnetic Survey

(1) Total Magnetic Force

Total magnetic force was measured in conjunction with the bathymetric survey, which was performed at intervals of 2nm track lines. The influence of magnetic storms was not recognized during the survey, and we did not compensate for diurnal variation of the magnetic field. A remeasurement was carried out along the same track line in order to check an accuracy if data were uncertain.

A total magnetic force map (Fig. 3-3-1) was drawn by gridding the measured values of total magnetic intensity at 1,500m spacing. The contour intervals are set at 100nT.

The total magnetic intensity is within the range of 42,000 ~ 48,000nT and the general trend is low at the north and high at the south. These trends are consistent with the trends of the global geomagnetic field.

(2) Magnetic Anomalies

A magnetic anomaly map (Fig. 3-3-2) was drawn by obtaining the primary trend surface from the values of the total magnetic force and then determining the residual between the total magnetic force and the trend surface. A magnetic anomaly map based on the residual between the total magnetic force and the International Geomagnetic Reference Field (IGRF) is shown in Figure 3-3-3.

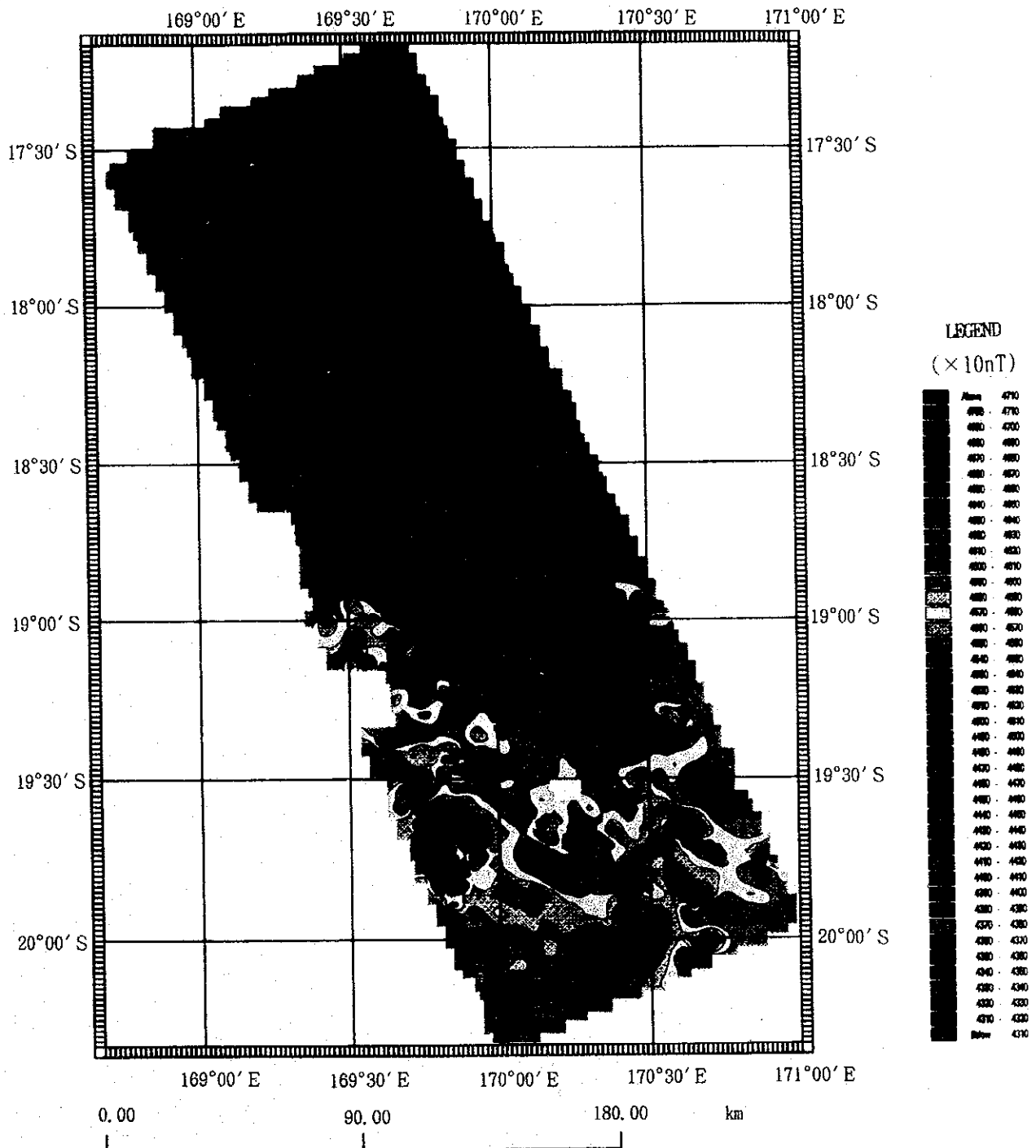


Figure 3-3-1 Total magnetic force map produced from the data of measured total force value gridded at a 1.5-km Spacing.
 Center labels are in nanoteslas (nT), and contour interval is 100nT

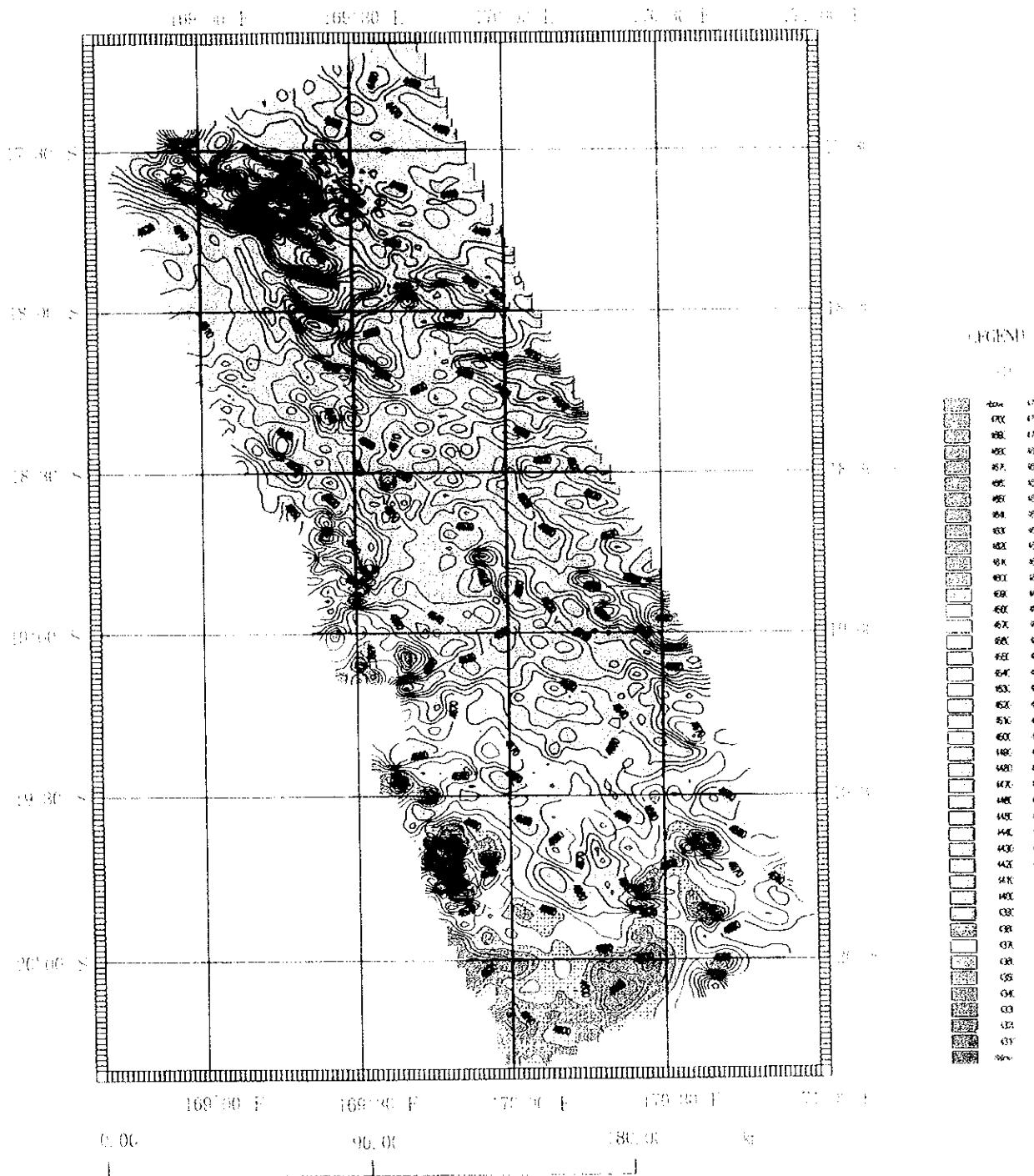


Figure 3-3-1 Total magnetic force map produced from the data of measured total force values gridded at a 1.5-km spacing. Center labels are in nanoteslas (nT), and contour interval is 4 nT.

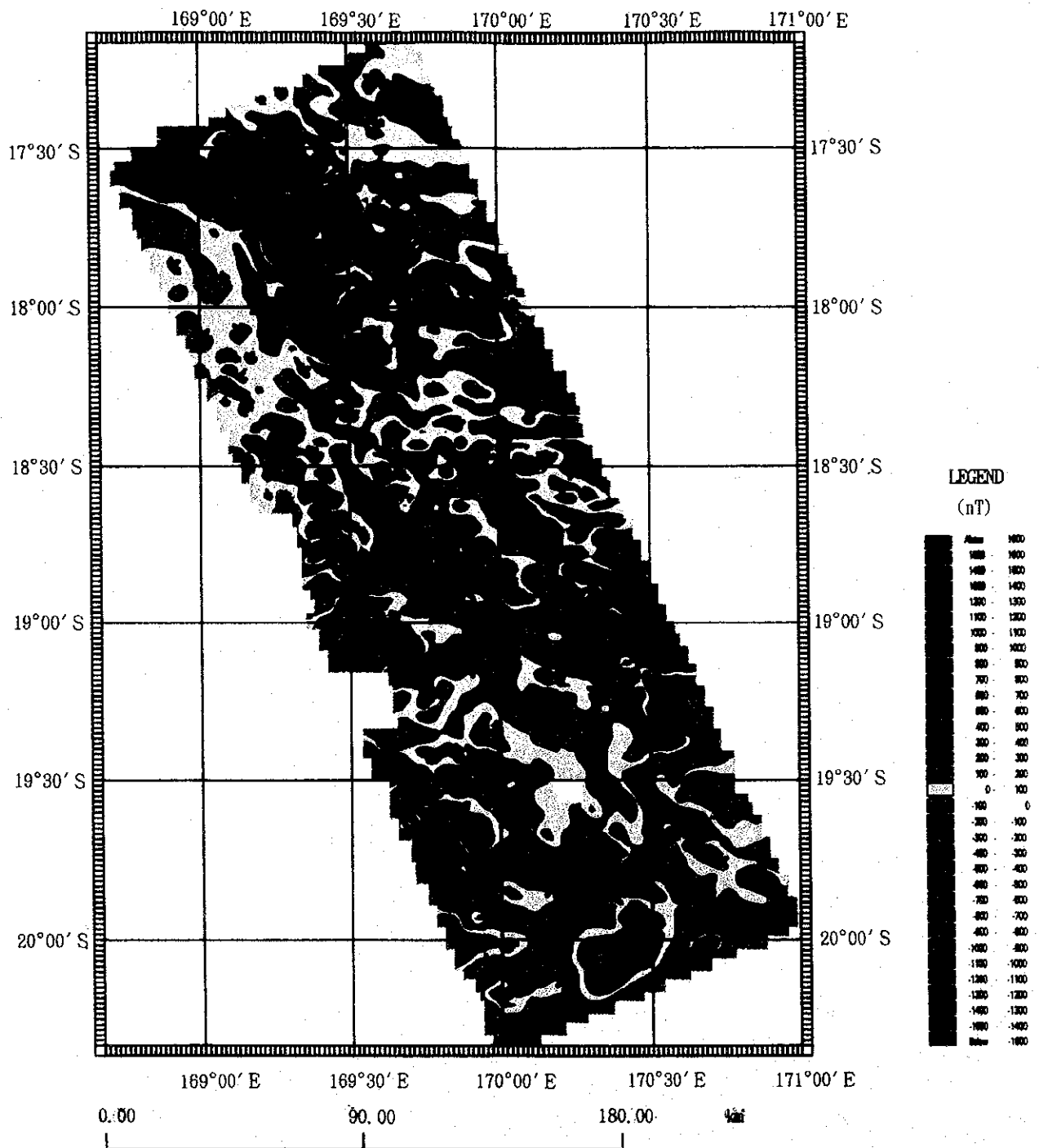


Figure 3-3-2 Magnetic Anomaly Map Produced from the Data Gridded at a 1.5-km Spacing. Contour interval is 100nT

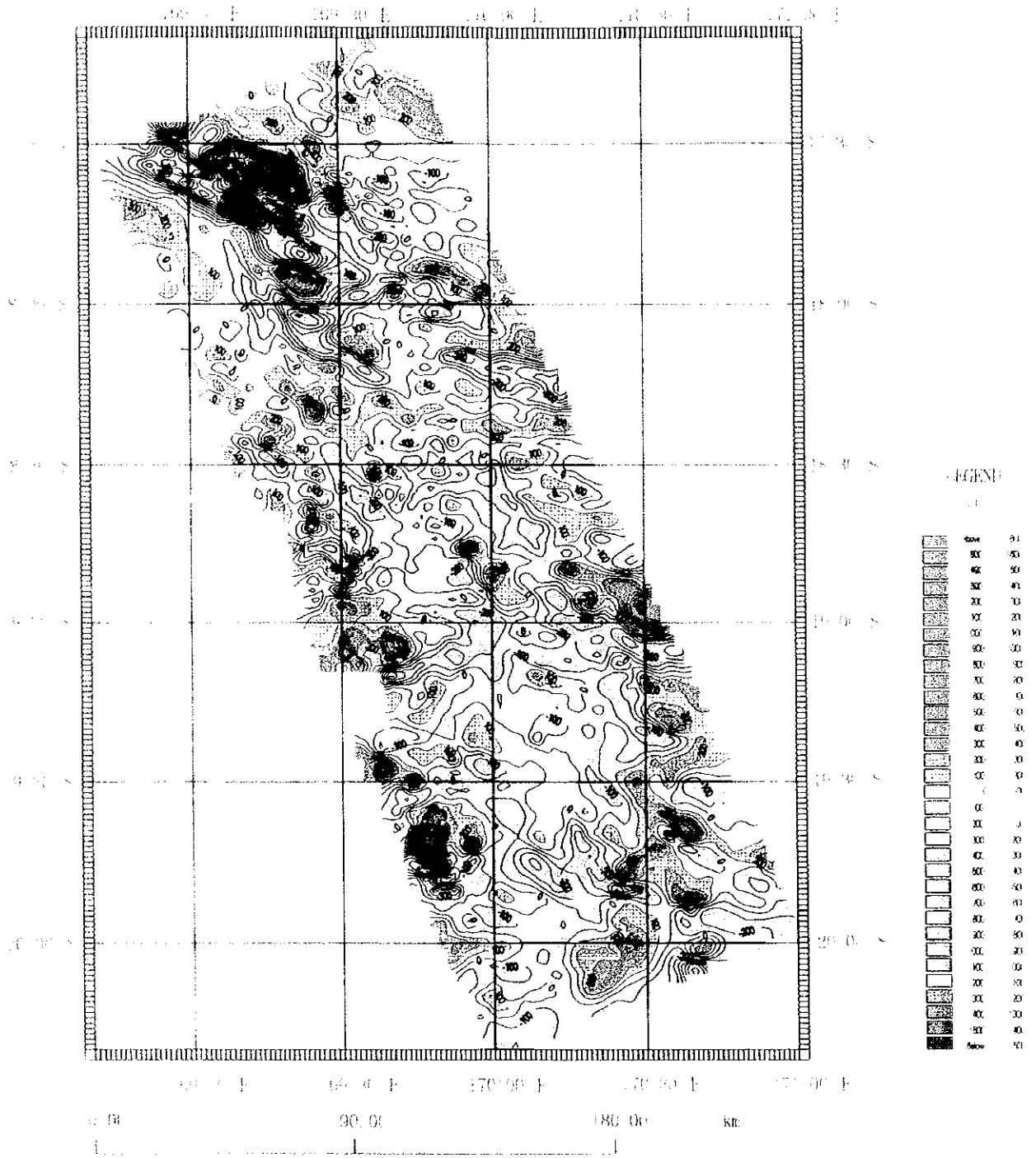


Figure 3.3-2 Magnetic Anomaly Map Produced From the Data Gridded at a 1.5 km Spacing
Contour interval is 100nT

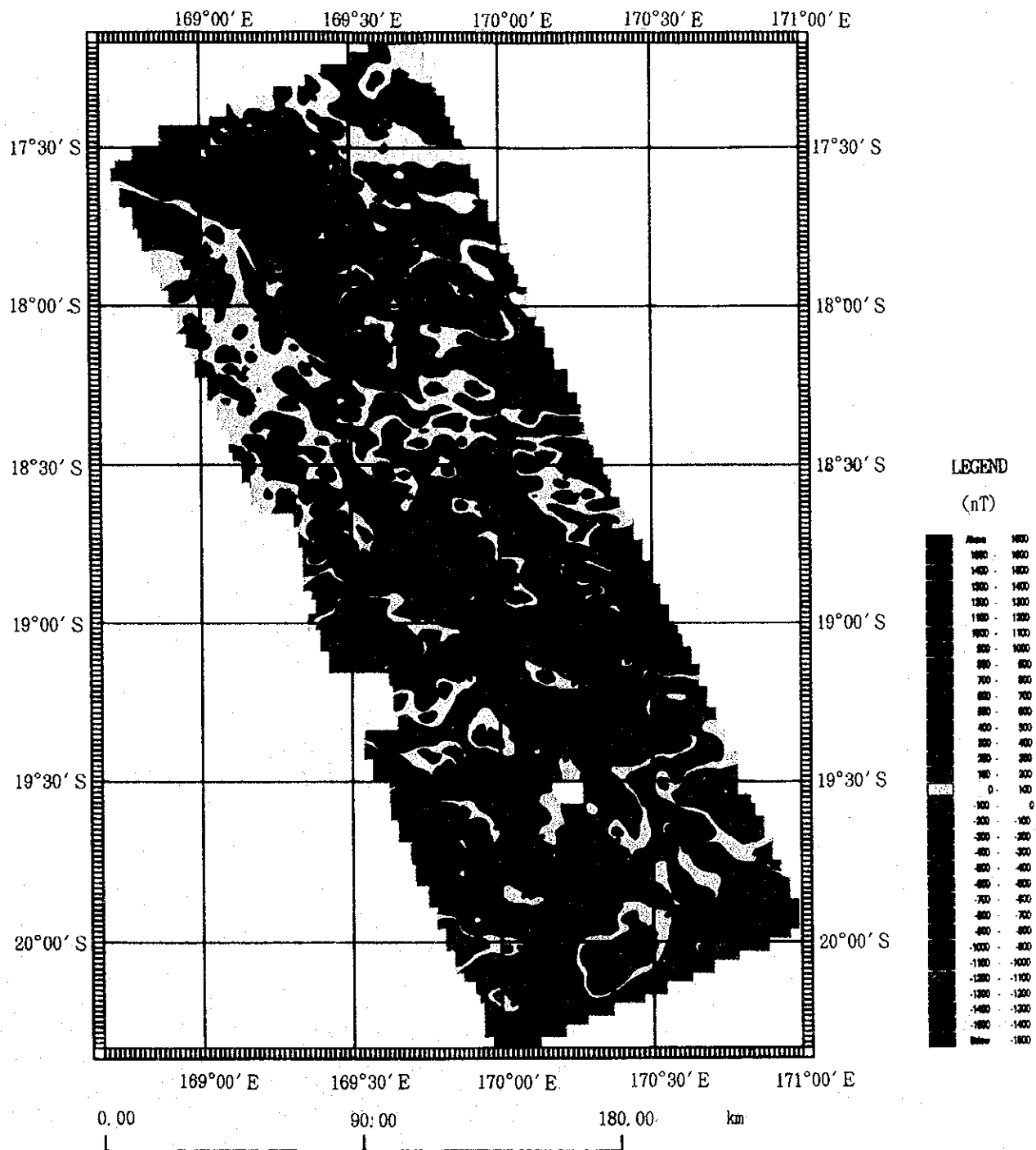


Figure 3-3-3 Magnetic Anomaly Map Produced from the Data Gridded at a 1.5-km Spacing. Contour interval is 100nT

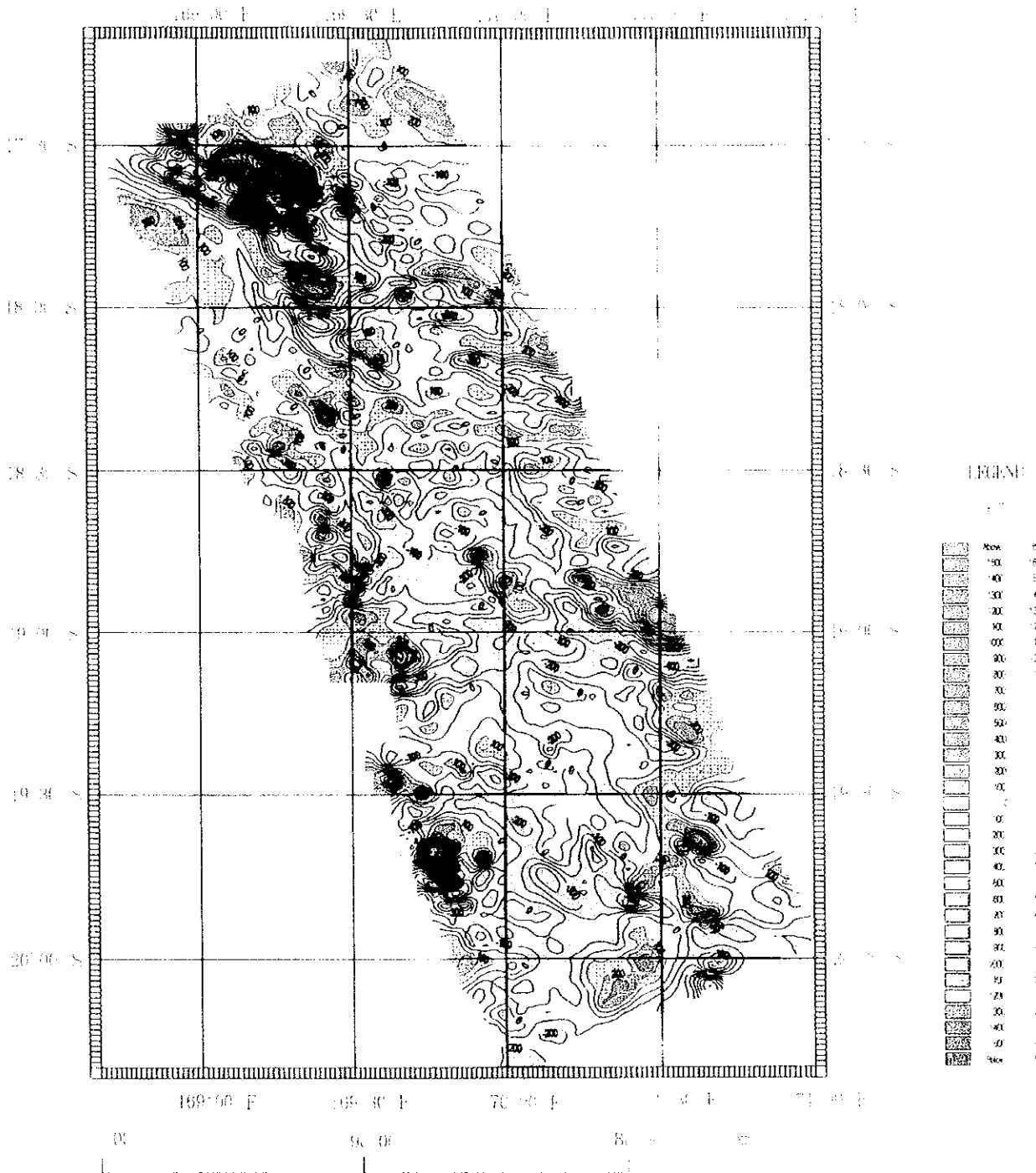
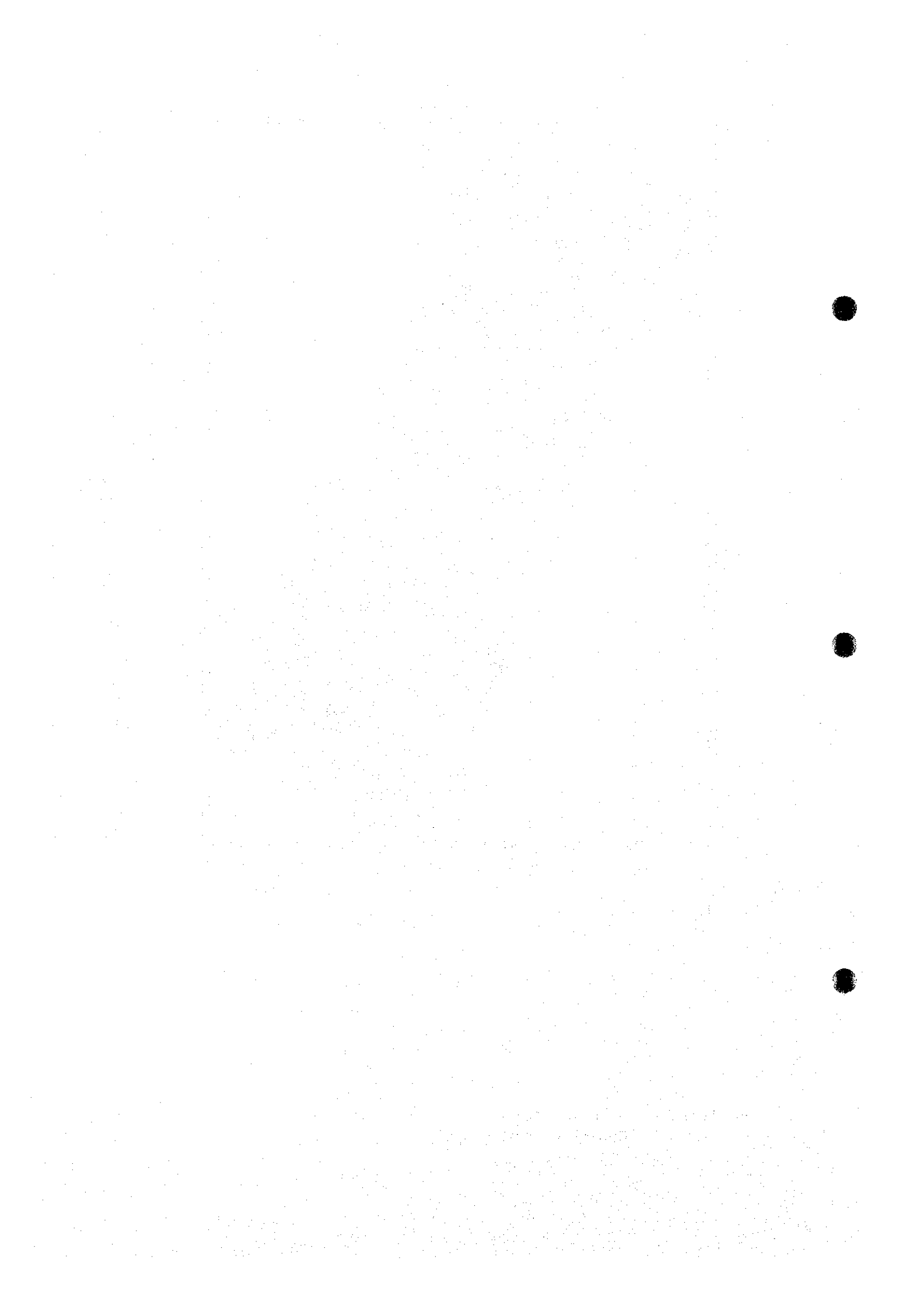


Figure 3-3-3 Magnetic Anomaly Map Produced From the Data Added at a 1.5 km Spacing. Contour interval is 100nT



When comparing the trend surface residual with the IGRF residual, we can see that they show a similar trend but the IGRF residual is about 100nT lower than the trend surface residual in the south.

A typical profile of magnetic anomalies is shown in Figure 3-3-4.

According to the magnetic anomaly map, magnetic lineation couldn't be defined in this survey area. In general, magnetic anomalies trending N60° W are prominent in the northern part of the survey area.

Some dominant magnetic anomaly in this area are further described as follows.

1) Magnetic anomalies in the northern part of the Vate Trough

Magnetic anomalies, trending ESE ~ WNW, are spreading in the northern part of the Vate Trough.

These anomalies are normally magnetized anomalies with an amplitude of -1,700 ~ +1,400nT.

Topographically, this area is a depression, so it is inconceivable that this magnetic anomaly is caused by topography. We therefore conclude that this is a magnetic anomaly concomitant with the tectonic line. Furthermore, there are magnetic anomalies that parallel and traverse this magnetic anomaly.

2) Magnetic anomalies on the border between the Vate Trough and the Erromango Basin

There are positive anomalies on the border between the Vate Trough and the Erromango Basin. These anomalies are positively magnetized linear anomalies with amplitude of +100 ~ +500nT and traverse the Vate Trough and the Erromango Basin from east to west.

These magnetic anomalies seem to correspond to the tectonic line but we cannot verify this from the topography.

3) Magnetic anomalies in the central ridge of the Erromango Basin

There are magnetic anomalies, trending ENE ~ WSW, in the center of the Erromango Basin. These are negative anomalies with amplitude of +300nT.

4) Magnetic anomalies in seamounts

Seamounts in this area show normally magnetized anomalies. However, the rather large magnetic anomalies, with an amplitude of -1,700 ~ +1,200 at 19° 45'S · 169° 45'E on the west of the Futuna Trough, are not caused by these seamounts but inferred to be caused by high magnetic rock.

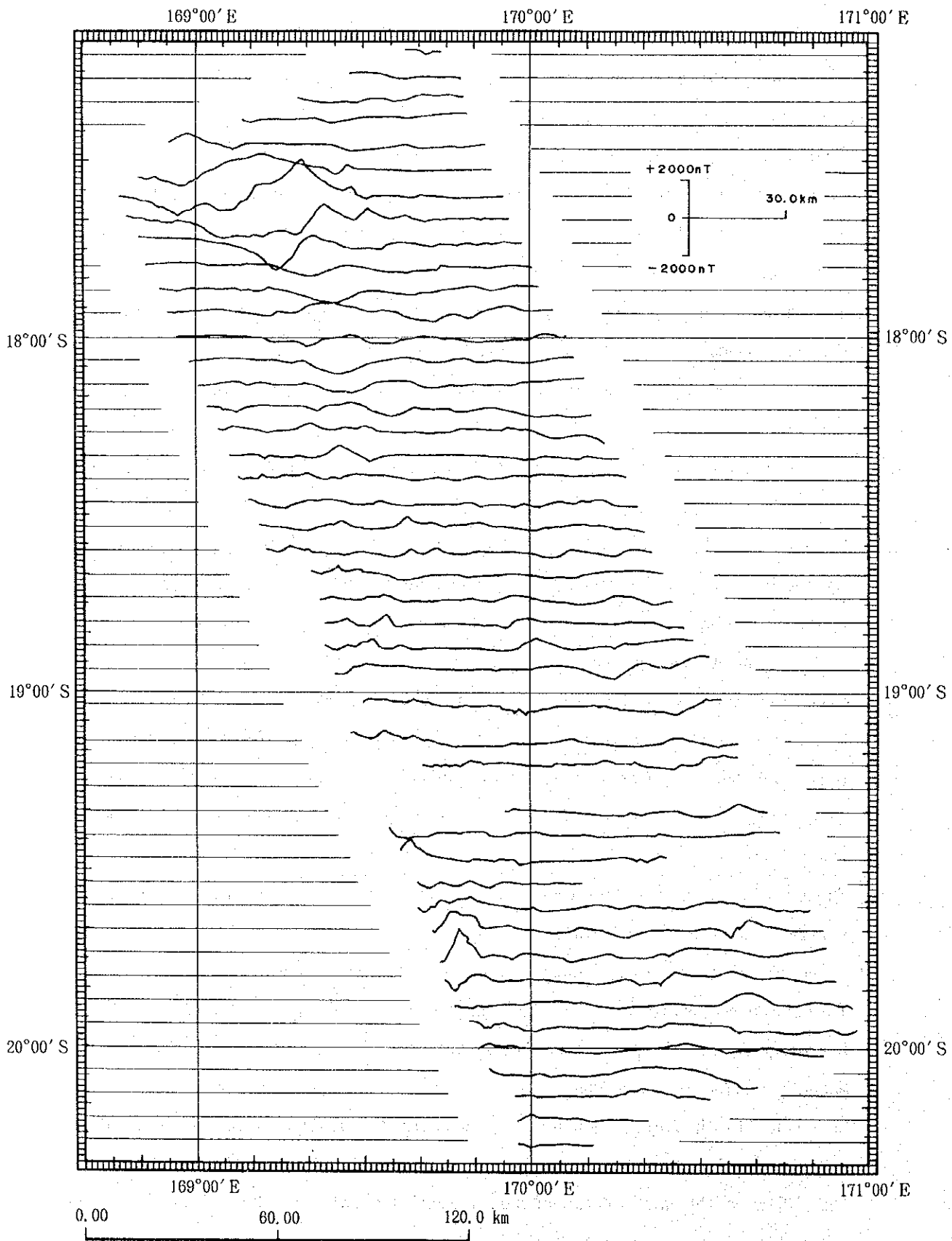


Figure 3-3-4 Magnetic anomaly profiles

(3) Reduction to the pole

Magnetic anomalies, caused by magnetic substances which are magnetized in the direction of the current geomagnetic field (positively magnetized substances), usually appear as a pair of magnetic anomalies, with a positive anomaly on the north of the magnetic substance and a negative anomaly on the south in middle and low latitudes of the Southern hemisphere. On the other hand, a single positive magnetic anomaly appears right above magnetic substances in the polar regions. Accordingly, we can easily compare these anomalies with topography and geology as well as calculate three-dimensional structure.

The difference in latitude between the north tip and south tip of the survey area is 190', which is rather large, and the dip varies from 45.5° S at the southwestern tip to 40.1° S at the northeastern tip. Accordingly we drew a Reduction to the Pole Map (Fig. 3-3-5) by adopting a 43° S dip in the central part of the survey area.

According to the Reduction to the Pole Map, magnetic anomalies trending NNW-SSE and NW-SE are emphasized. Positive anomalies are prominent in the northern part of the area and negative anomalies are prominent in the southern part of the area. Furthermore, correlation with submarine topography was indistinct in the IGRF Residual Magnetic Anomalies Map, but positive correlation between topographic heights of the island-arc marginal parts-- tops of fault scarps and seamounts-- and high reduction to the pole became clear. Especially, positive anomalies are eminent on the seamounts and sea knolls scattered about the central through southern parts of the area.

The features of this distribution of reduction to the pole are as follows:

- ① Positive anomalies with relatively large amplitude are prominently distributed in the northern part. The western, eastern and southeastern parts are regions of positive anomalies with small amplitude including a group of independent positive anomalies. But central through southern parts assume regions of negative anomalies with small amplitude. Different distributions of magnetic anomalies are shown on the Vate Trough, Erromango Basin and Futuna Trough within the Coriolis Troughs.
- ② Positive anomalies with the largest amplitude in the survey area are distributed in the deepest part of the Vate Trough, trending NW-SE in the northern part of the area. Positive anomaly groups, and with small amplitude

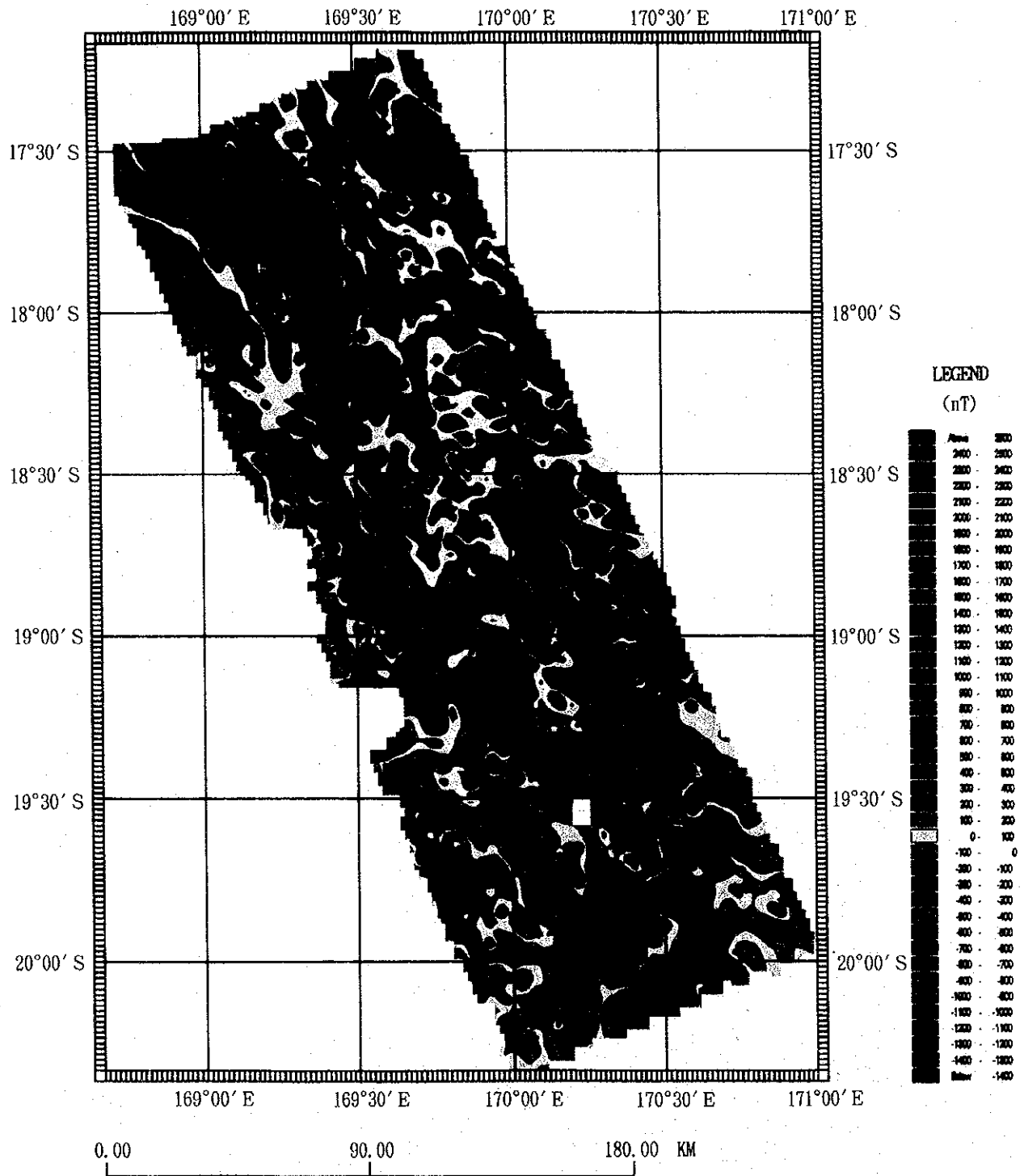


Figure 3-3-5 Reduction to the pole anomaly map derived from the total magnetic force value. Contour interval is 100nT

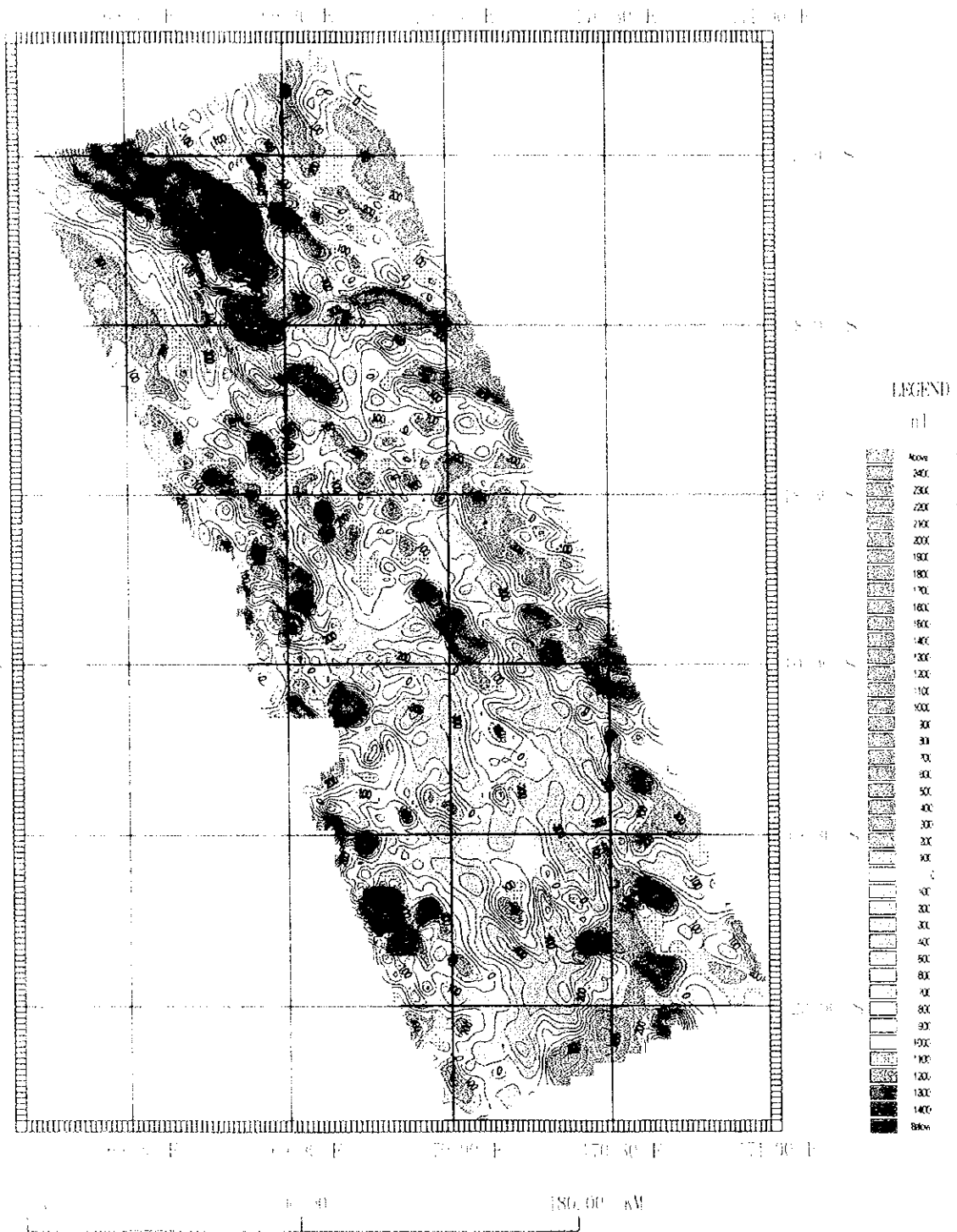


Figure 3.3.4 Reduction to the pole anomaly map derived from the total magnetic force value. Contour interval is 100nT

corresponding to the top of the fault scarp, are identified trending NNW-SSE at the east and west ends of the Vate Trough.

- ③ Positive anomalies, trending NNW-SSE, are distributed on the top of the fault scarp on the east of the Erromango Basin, but, on the whole, the region in and around the Erromango Basin including the eastern slopes of the fault scarp shows little variation of polar magnetism.
- ④ In the southern part of the Futuna Trough, positive anomalies with small amplitude are recognized at an area close to Futuna Island on the bottom of the Trough, but as in the case of the Erromango Basin, this region, including the top of the fault scarp on the east, shows little variation in polar magnetism.
- ⑤ Different distribution of reduction to the pole is shown in the topographically convex part between these troughs and the basin. A group of positive anomalies, trending NW-SE, continuing from the Vanuatu Island arc side are recognized between the Vate Trough and the Erromango Basin and small scale positive anomalies, trending NW-SE, are recognized between the Erromango Basin and the Futuna Trough.
- ⑥ A group of independent positive anomalies is distributed at the southwestern and southeastern ends of the survey area which roughly coincides with the location of seamounts.

(4) Magnetization Distribution

In the analysis of three dimensional magnetization distribution, we approximated the distribution of magnetic substances existing under the sea-floor to three-dimensional models composed of a gathering of prisms, thus obtaining the prismatic intensity of magnetization by the magnetic inversion method.

For this purpose we defined the top of every prism as the sea-floor surface and the lower surface as 20km below the sea level.

A Magnetization Distribution Map is shown in Figure 3-3-6. Features of the distribution of magnetization are as follows:

① On the whole, magnetization distribution

On the whole, magnetization distribution within the survey area can be summarized into two characteristic zones. One is a zone of high magnetization distributed in the northern part of the survey area including the Vate Trough, the western tip corresponding to the eastern slope of the Vanuatu island arc and the southeastern

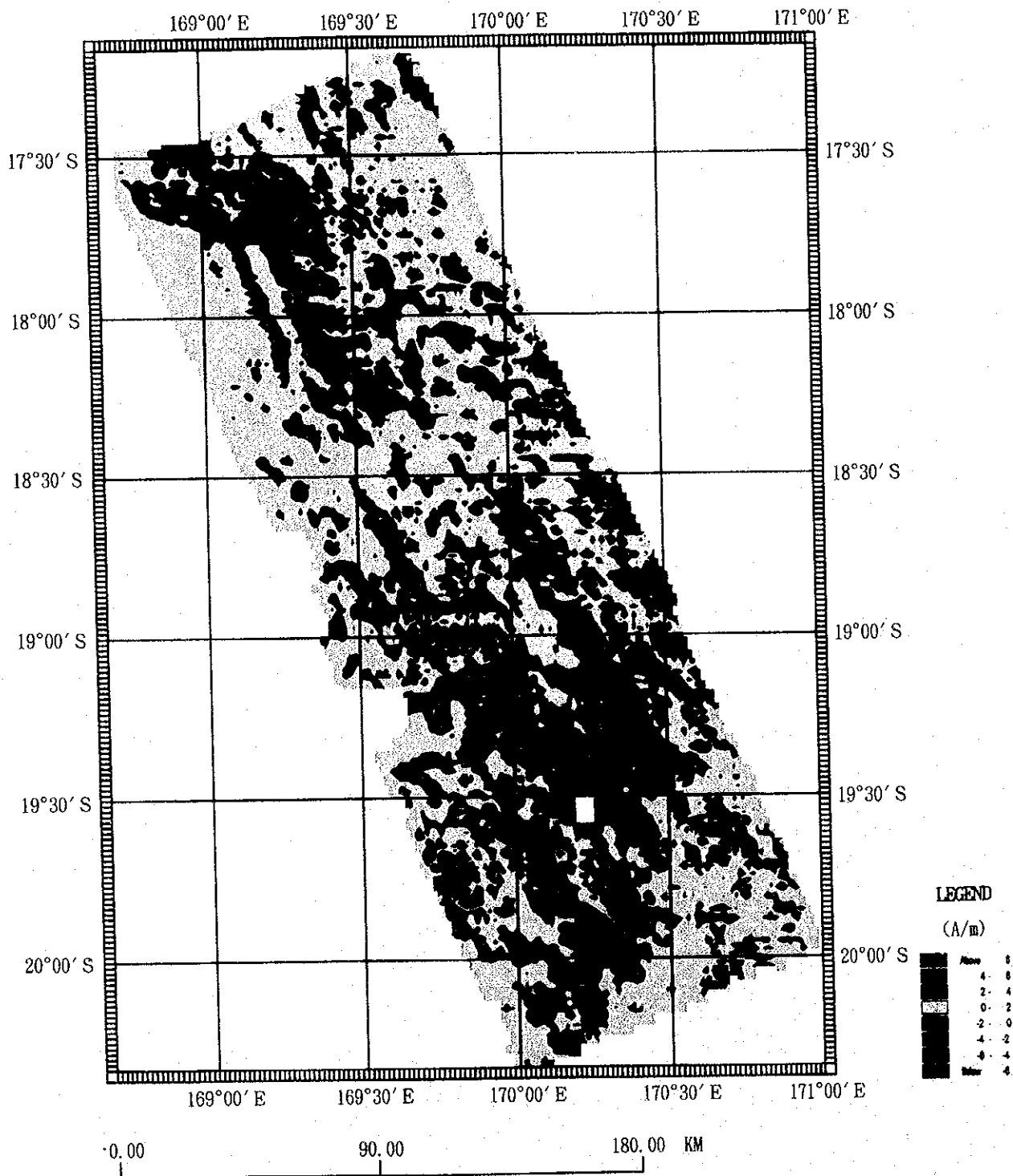


Figure 3-3-6 Magnetization distribution map from three-dimensional inversion solution of gridded bathymetric and magnetic anomaly data. Contour interval is 2-A/m

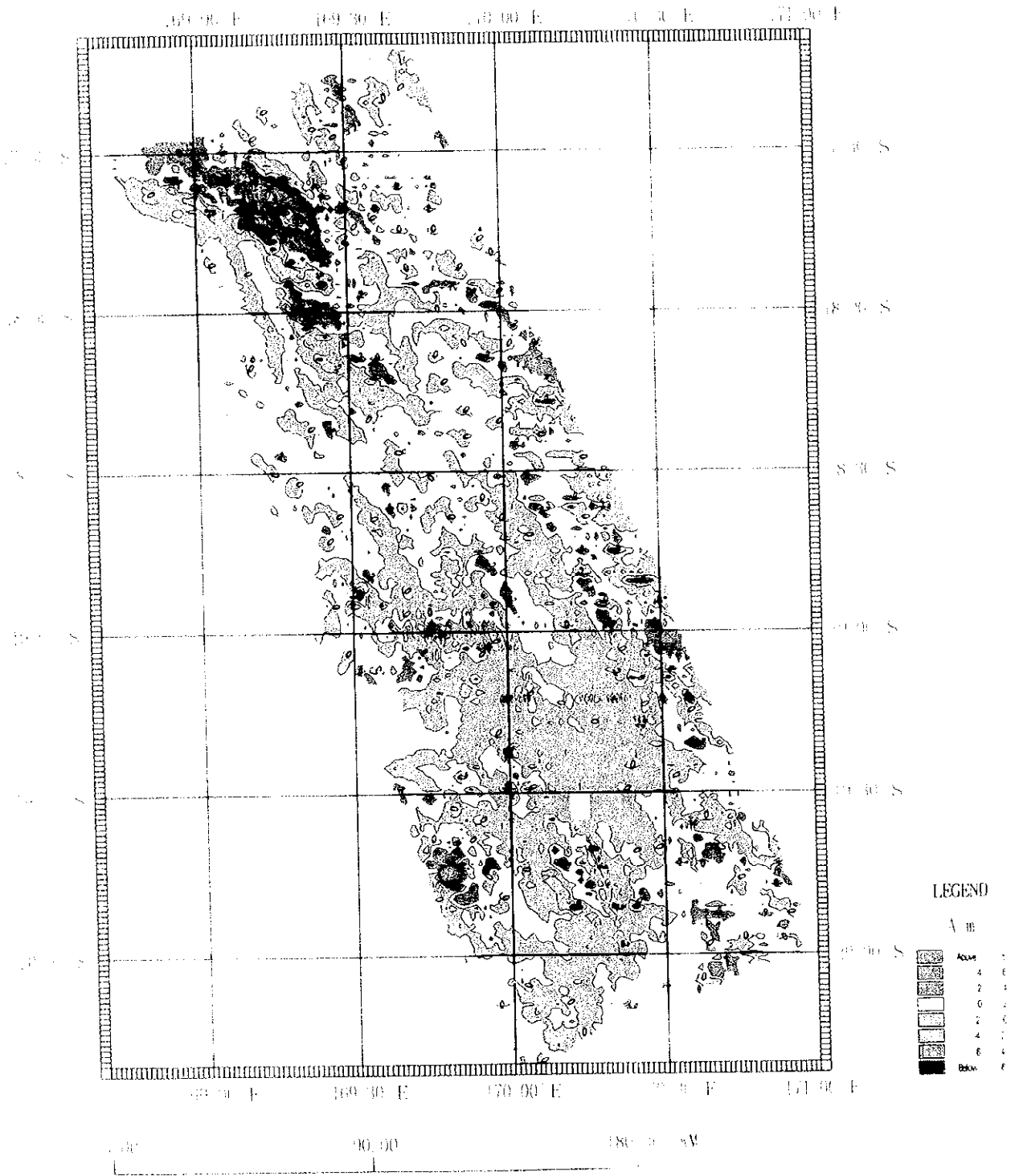


Figure 3-3-6 Magnetization distribution map from three dimensional inversion solution of gridded bathymetric and magnetic anomaly data. Contour interval is 2-A/m

part. The other is a zone with low magnetization distributed in and around the Erromango Basin and Futuna Trough in the central and southern parts of the survey area. These zones reflect differences of geological structure between the Vate Trough and the Erromango Basin/Futuna Trough. Among the former, the zones with high magnetization in the northern and northeastern part of the area trend from NNW-SSE to NW-SE.

Negative magnetization is distributed in the whole district of the Erromango Basin/Futuna Trough in the central and southern parts and the Vate Trough in the northern. Each of them shows an intensity of magnetization of more than $-2A/m$. The region of negative magnetization is not entirely magnetized inversely. It is supposed that this reflects the fact that the major portion of the central and southern part is made up of non-magnetic substances and that the negative magnetization in the northern part is an apparent negative magnetization generated by the structure of magnetic substances (inclining to the east).

② Magnetization distribution in and around the Vate Trough

A high magnetization zone, trending NW-SE, with an intensity of more than $2A/m$, is distributed in the Vate Trough. This zone is distributed from the northwestern end of the survey area. High magnetization zones, though on a small scale with an intensity of more than $2A/m$, line up roughly in the same direction in the central and southern parts of the Vate Trough. The high magnetization zone in the northern part corresponds to younger lava around the sea-floor (Price, et al., 1993). Small-scaled high magnetization zones in the central and southern parts are inferred to be caused by a ridge with new lava.

Low magnetization, trending SN, of less than $1A/m$ is recognized at the western end of the Vate Trough, coinciding with a convex part of the seafloor topography. The west side of the Vate Trough is a low magnetization zone of less than $1.5A/m$. It corresponds to volcanic rocks composing the Vanuatu island arc. On the other hand, the entire eastern part of the Vate Trough is a positive magnetization zone in which low magnetization of less than $1A/m$, roughly trending NS, is distributed along fault scarps and magnetization of more than $1.5A/m$, trending NNW-SSE ~ NW-SE, is distributed on the eastern slopes.

Most of the area between the Vate Trough and Erromango Basin, to the south of the Vate Trough, is a region with positive magnetization, in which, positive magnetization trending NW-SE is arranged, coinciding with convex parts

(seamounts) of the seafloor topography.

③ Magnetization distribution in and around the Erromango Basin/Futuna Trough.

Around the Erromango Basin and Futuna Trough is, unlike the periphery of the Vate Trough, an area practically without magnetization, and it is supposed that the magnetic structure of this area is totally different.

The intensity of magnetization within the Erromango Basin is nearly 0 except for small-scaled positive magnetization appeared near the Trough axis. It is a region almost without magnetization. Furthermore, no positive magnetization is recognized around the ridges in the Basin. Positive magnetization, trending NW-SE to NNW-SSE, is distributed on the top of the fault scarp on the east but the magnetization disappears on the eastern slopes in the east, while small-scaled positive magnetization trending NNW-SSE is scattered further east.

Small-scaled areas of positive magnetization corresponding to rises of the seafloor topography appear between the Erromango Basin and Futuna Trough. On the other hand, the Futuna Trough is, just like the Erromango Basin, a region almost without magnetization except in the region from the vicinity of the Trough axis to the eastern walls where magnetization of about 1.5A/m is identified. Fault scarps including Futuna Island and slopes on the east are regions totally without magnetization. As mentioned above, the Erromango Basin and Futuna Trough present an entirely different magnetic structure from the Vate Trough including the Basin/Trough and eastern slopes of the fault scarps although these formations are all in the same Coriolis Troughs. It is presumed that this reflects differences of magmatism.

Positive magnetization trending NNW-SSE is identified to the northwest of the Erromango Basin. This magnetization coincides with rises of the seafloor topography stretching from the Vanuatu island arc. Isolated areas of positive magnetization are distributed around 19° 05'S on the eastern slope of the Vanuatu island arc west of the Erromango Basin. But these areas of magnetization do not coincide with the top of the seamount, which leads us to believe that there is great potential of demagnetization on the south of the seamount.

Small-scaled positive magnetization is distributed intermittently from the Vanuatu island arc side to the area between the Erromango Basin and Futuna Trough around 19° 30'S. The intensity of this magnetization becomes weaker on the east. Each area of magnetization roughly coincides with the location of each seamount. The

intensity of magnetization decreases as we approach the Basin and Trough.

Three isolated areas of positive magnetization are distributed around 19° 30'S, west of the Futuna Trough. Two of them to the north correspond to seamounts. The southern area of magnetization is supposed to be caused by a latent seamount.

④ Magnetization distribution on seamounts in the south-eastern part

Isolated areas of positive magnetizations are scattered on the south and eastern sides, outside the Futuna Trough, roughly coinciding with the location of seamounts. The intensity of magnetization has a tendency to decrease toward the north.

(5) Magnetic structure map

A magnetic structure map shows the following structures inferred from the Reduction to the Pole Map and Magnetization distribution Map.

- Non-magnetized zone a scope representing non-magnetism
- A fault a place showing the maximum incline of the reduction to the pole
- A magnetic lineament (a line of magnetic discontinuity) ...
a line linking continuous and positive reduction to the pole
- A seamount chain a line linking positive magnetic anomalies of seamounts in the southeastern part of the survey area

Characteristics of the magnetic structure in Figure 3-3-7 are as follows:

- ① Magnetic lineation representing sea-floor spreading is not recognized within the survey area.
- ② Magnetic lineaments trending NNW-SSE to NW-SE are prominent in the northern part of the survey area.
- ③ A fault is inferred from the distribution of reduction to the pole on the eastern side of the Vate Trough and Erromango Basin. But, it is difficult to infer the existence of a fault on the eastern side of the Futuna Trough.
- ④ Rock masses with high magnetism are distributed in the Vate Trough, so the Vate Trough is a normally magnetized region. In and around the Erromango Basin and Futuna Trough is a non-magnetized region. These facts indicate entirely different magnetic structures in these two regions.

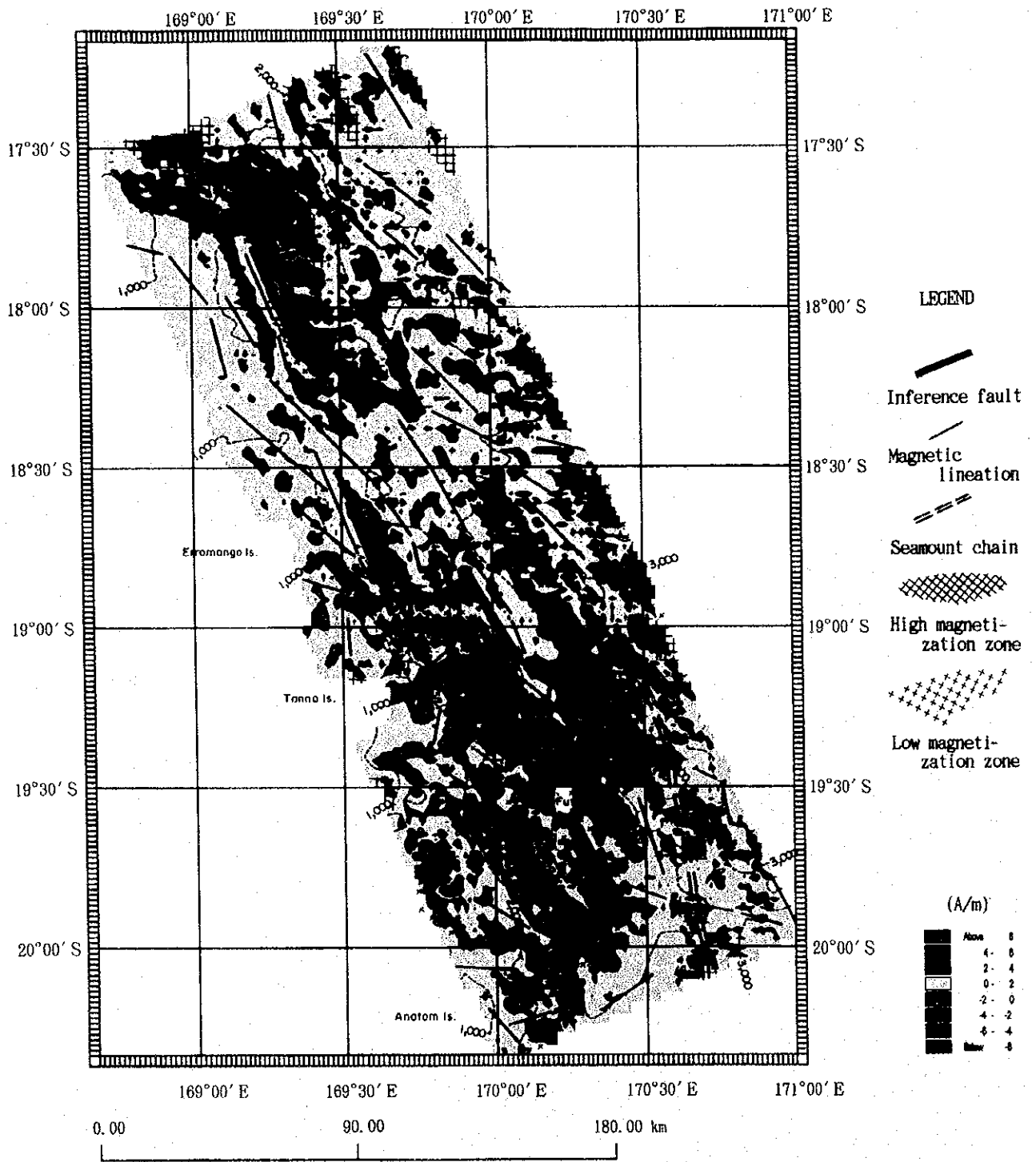


Figure 3-3-7 Magnetic Structural Map

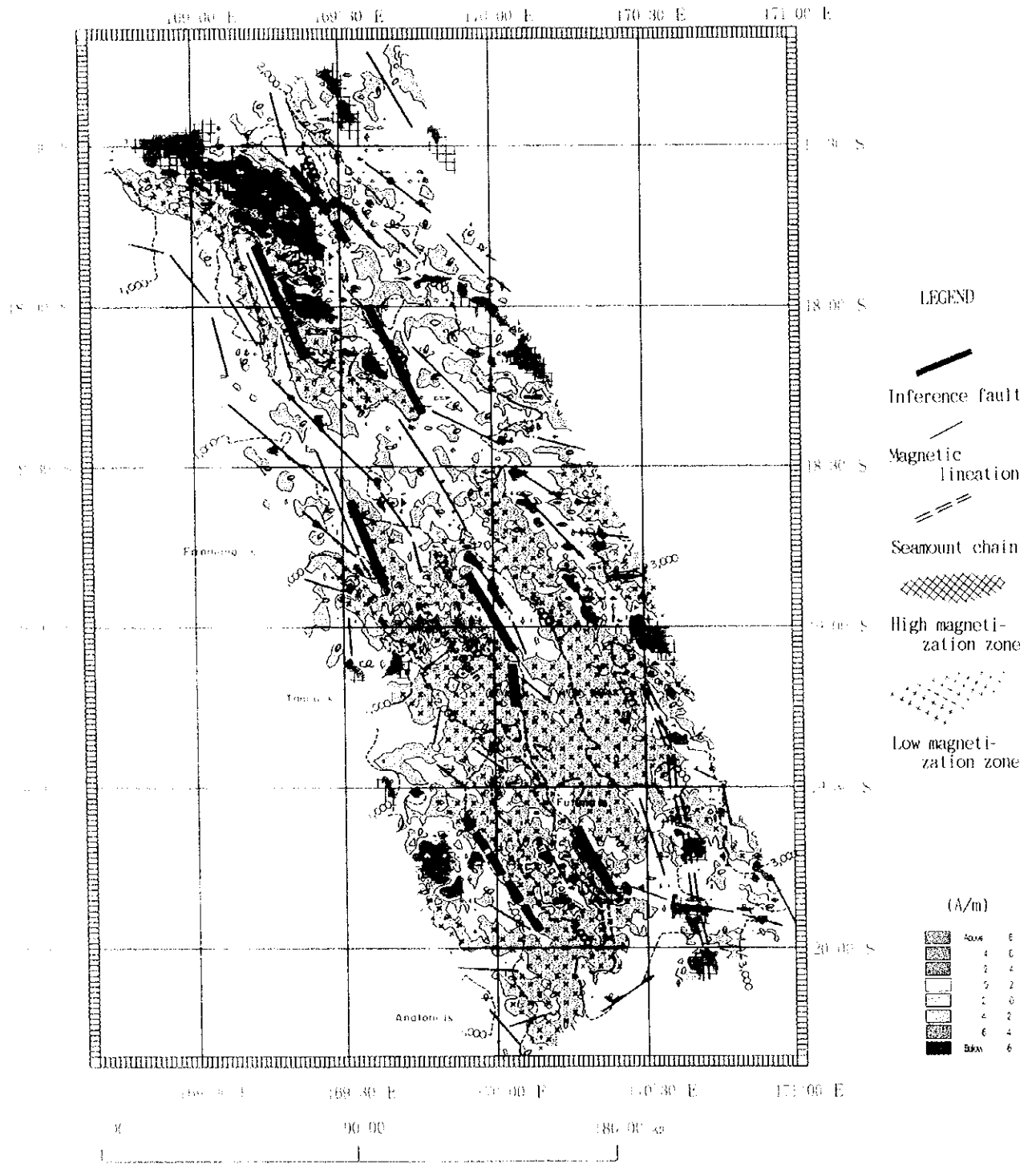


Figure 3-3-7 Magnetic Structural Map

- ⑤ The volcanic front in the western part of the survey area is a highly magnetized region and rock masses with high magnetism are distributed on the seamounts but some of the seamounts are demagnetized.
- ⑥ A seamount chain in the southeastern part of the survey area is normally magnetized and its magnetism has a tendency to decrease in the northern part.

3-4 Geological Structure

(1) Geological Structure

This fiscal year's survey area is located in the back arc area of the southern part of the New Hebrides arc. As a result of spreading of the back arc, the Coriolis Trough is located in the center of the area. The Coriolis Trough occupies an area 20 ~ 30nm away from the volcanic front. The Coriolis Trough is a rectilinear depression about 20nm wide and more than 160nm long. The relative depth of its base is about 1,500m. Its principal axis trends N20° W.

The southern tip (to the south of 20° S) is excluded from the survey.

The survey was conducted on the most part of the Coriolis Troughs and arc platform slopes from the neighborhood of the volcanic front, where the depth is less than 700m, to the North Fiji Basin, the depth of which exceeds 3,000m. A geological structure map based on a submarine topographic map and an acoustic reflection image map are shown in Figure 3-4-1-1.

1) The Vate Trough

The Vate Trough is located to the east of Efate Island.

Its major axis, trending N35° W, is 60nm and its maximum width is about 28nm. Its relative depth is about 1,300 to 1,500m. The scale of the Vate Trough is the largest among the three basins. Ridge-shaped topography, trending N20° W, with a relative height of 800 ~ 1,300m divides the basin into two at around 18° 05'S · 169° 10'E in the basin. This ridge is inferred to be a fragment of an island arc. Steep cliffs, showing a normal fault, occur on the east and west slopes of the ridge and on the island side (the west side), which is opposite to the east and west slopes, as well as on the basin slopes on the marginal-sea side (the east side). Distribution of sediments, supplied from the land to the basin surrounded by the ridge-shaped topography and the plateau on the island arc side, is recognized from the MBES acoustic reflection image and SBP records.

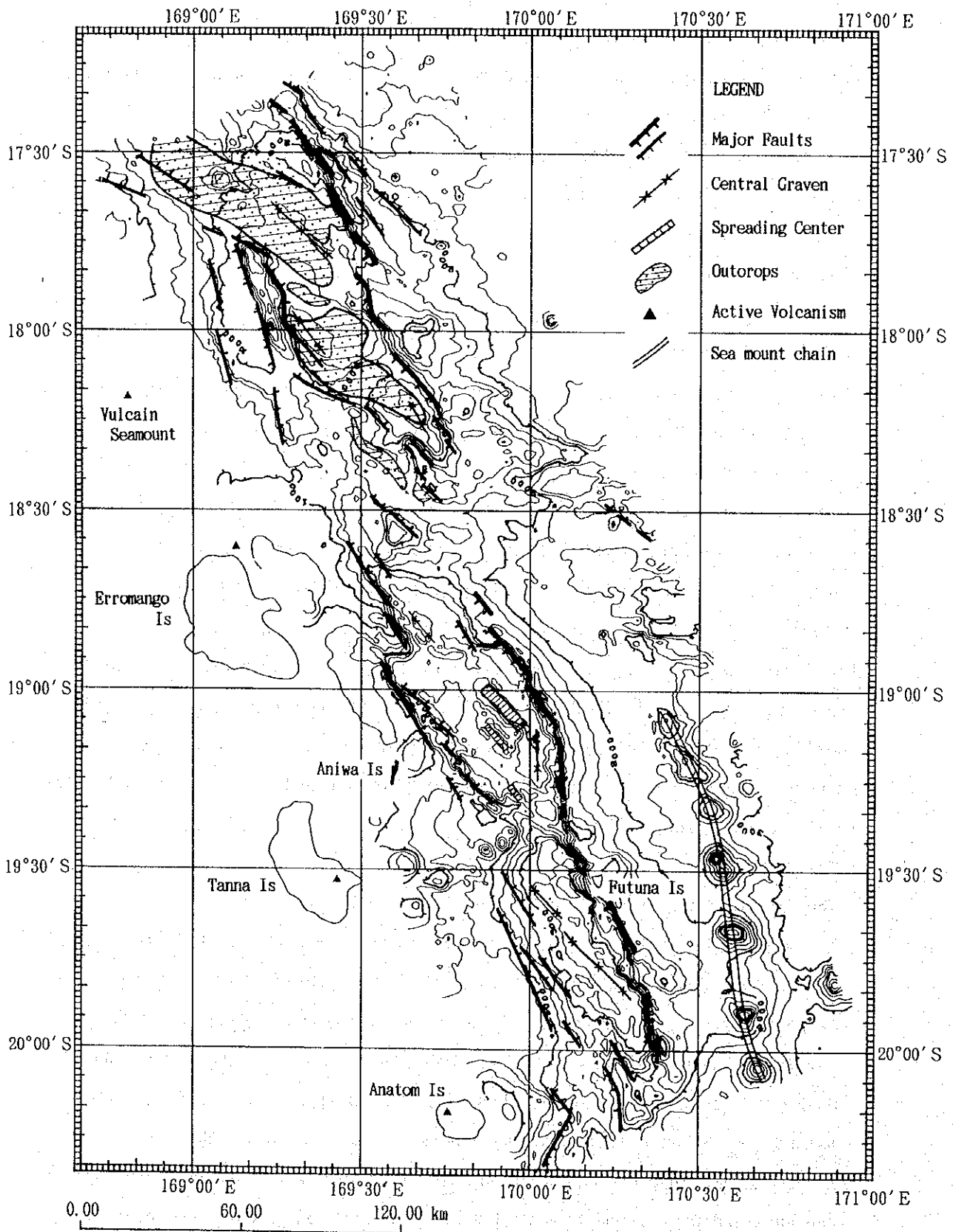


Figure 3-4-1-1 Geological Structural Map

Extensive distribution of rock on the island arc slopes and the basin floor on the north of the above-mentioned ridge, and a basin on the east are also identified from the MBES acoustic reflection image and SBP records. Some of these are identified by FDC.

A depression, constituting the center of the opening of the Trough and showing the maximum depth, is divided by a plateau-shaped rise formed by an intrusion of $18^{\circ} 30'S - 169^{\circ} 30'E$, but it has a major axis trending $N40^{\circ} W$ that transverses the trough's axis diagonally.

Rises, depressions and steep cliffs facing them are distributed around a line (trending $N50^{\circ} W$) linking the seamounts with calderas at $17^{\circ} 35'S, 169^{\circ} 05'E$ and the discontinuous part in the eastern margin of the Trough at $17^{\circ} 51'S, 169^{\circ} 38'E$. This part is inferred to be a part of the trough that bends toward the west from the fact that this part coincides with the magnetic anomaly zone. The depression's major axis trends $N55^{\circ} W \sim N50^{\circ} W$, which coincides with the stretching direction of the trough. This place is considered to be the most active part at present.

2) Between the Vate Trough and the Erromango Basin

The tip of the rise continuing from Erromango Island forms a plateau at the sill between the Vate Trough and the Erromango Basin and is a part of the arc platform. There is a possibility that the part around $18^{\circ} 25'S, 169^{\circ} 35'E$ is the part that starts to open as a trough from the fact that it forms a depression with a major axis trending $N50^{\circ} W$ and a relative depth of about 200 ~ 500m, and that the part of the major axis position are formed small rise of outcrops of rocks.

3) The Erromango Basin

The Erromango Basin is located to the east of Erromango Island and Tanna Island. Its major axis is 45nm and its width is 17nm. The major axis trends $N38^{\circ} W$. Water depth at the top of west cliff is about 800m and at the top of east cliff about 900m. The relative depth to the basin floor is about 2,000m. Slopes cascading from the arc platform to the basin on the east and west sides assume normal faults.

Ridge-shaped rises, formed by 2 ~ 3 layers of normal faults and holding a graben-shaped depression, stretch in the direction of $N47^{\circ} W$, from which we can see that the trough has expand in the direction of N-S in two or three stages.

These ridge-shaped rises and a graben-shaped depression form a line and a depression with an N-S axis is formed at the front and rear parts of the line. From this, we can infer that the trough spread in the E-W direction after the ridge-graben had been formed. The basin floor appearing on the MBES acoustic reflection image is extensively covered by sediments. The eastern part especially, assumes a smooth surface which infers that the sediments are thick. Strong reflection showing the existence of outcrops on the ridge-shaped rises is also obtained and some of the outcrops are identified by FDC.

4) Between the Erromango Basin and the Futuna Trough

The area between the Erromango Basin and the Futuna Trough is a sill, the depth of which is about 2,000m, with the ridge-graben structure in the Erromango Basin stretching to the sill with lateral deviation.

A depression, with the relative depth of 200 ~ 300m, considered to be influenced by a tectonic line, trending SW-NE and represented by a chain of seamounts continuing from the southern part of Tanna Island, as well as by the Trough, is recognizable. Relatively strong reflections, appearing to be outcrops, are recognized on the MBES acoustic reflection image in most of the area except this depression.

5) The Futuna Trough

The Futuna Trough has a major axis of 38nm and a width of 17nm. Its major axis trends N18° W. Water depths at the top of west cliff are 1,800 ~ 1,900m and at its east cliff 1,400 ~ 1,500m. The depth of the basin floor is 3,200m. The Futuna Trough is slightly smaller than the Erromango Basin but its depth is deeper. Its east side is steep cliffs but the trough walls on the west side show lineaments- one of which parallels with the direction of the Trough's major axis, and the other transverses diagonally the Trough's major axis and parallels with the graben's axis that trends N40° W with relatively wide and terraced slopes.

According to the acoustic reflection image, these slopes are rock covered with sediments.

The trough bottom is also shaded. Places showing flat sea-floor with distribution of sediments are found in the southern part of the trough bottom.

The Trough axis deviates laterally and moves westward and southward of 20° S under the influence of the N50° E trending tectonic line.

A crank-shaped topography stretches to the SW in the southern Futuna Trough. Interpretation will differ due to the existence of this crank-shaped topography, but if we divide the Vate Trough into two narrow basins, south and north, then, each one of the four basins in the Coriolis Trough would have almost the same scale of 15 ~ 17nm wide and 38 ~ 45nm long. (It may have something to do with the activity, at intervals of 40 ~ 45nm, of volcanic fronts of the Vulcan Seamount, the east coast of the Erromango, Tanna and Anatonm).

The major axes of the basins trend N50° W, N42° W, N38° W and N18° W (in order of the location from north to south). It increases a tendency of trending north as the location moving south, while the axis of the graben -- which is considered to be the spreading center -- trends N50° W, N42° W, N47° W and N50° W, slightly increasing a tendency of trending west at the south. This has relevance to the Coriolis Trough's opening as a result of colliding with the DEZ's arc.

(2) MBES Acoustic Reflection Image

In order to identify the distribution of marine sediments, especially the situation of outcrops of rock masses spouted out concomitant with the spreading of rifts and the covering of sediments as a result of such spreading, an MBES Acoustic reflection Image Map (Fig. 3-4-2-1) was drawn using reflected sound pressures received from MBES beams. In the image, the higher part of the reflected sound pressure obtained from the sea-floor is expressed by black and the lower part by white. This chart is divided into the following three parts:

1. high sound pressure and a darker shade
2. uniformly low sound pressure and a lighter shade
3. changing sound pressure and a mottled shade.

From the results of FDC observation, we found that these represent outcrops of rock masses, surfaces of sediments and rock masses thinly covered with sediments. The part with a mottled shade, however, varies from darker to lighter according to the sediment coverage, degree of surface-roughness and so on.

Trends of the trough's major axes, such as N20° W, N70° W, N45° W and N55° W and a lineation that transverses them diagonally can be recognized from the acoustic image.

It also shows the prominent distribution of sediments in the whole area and rock

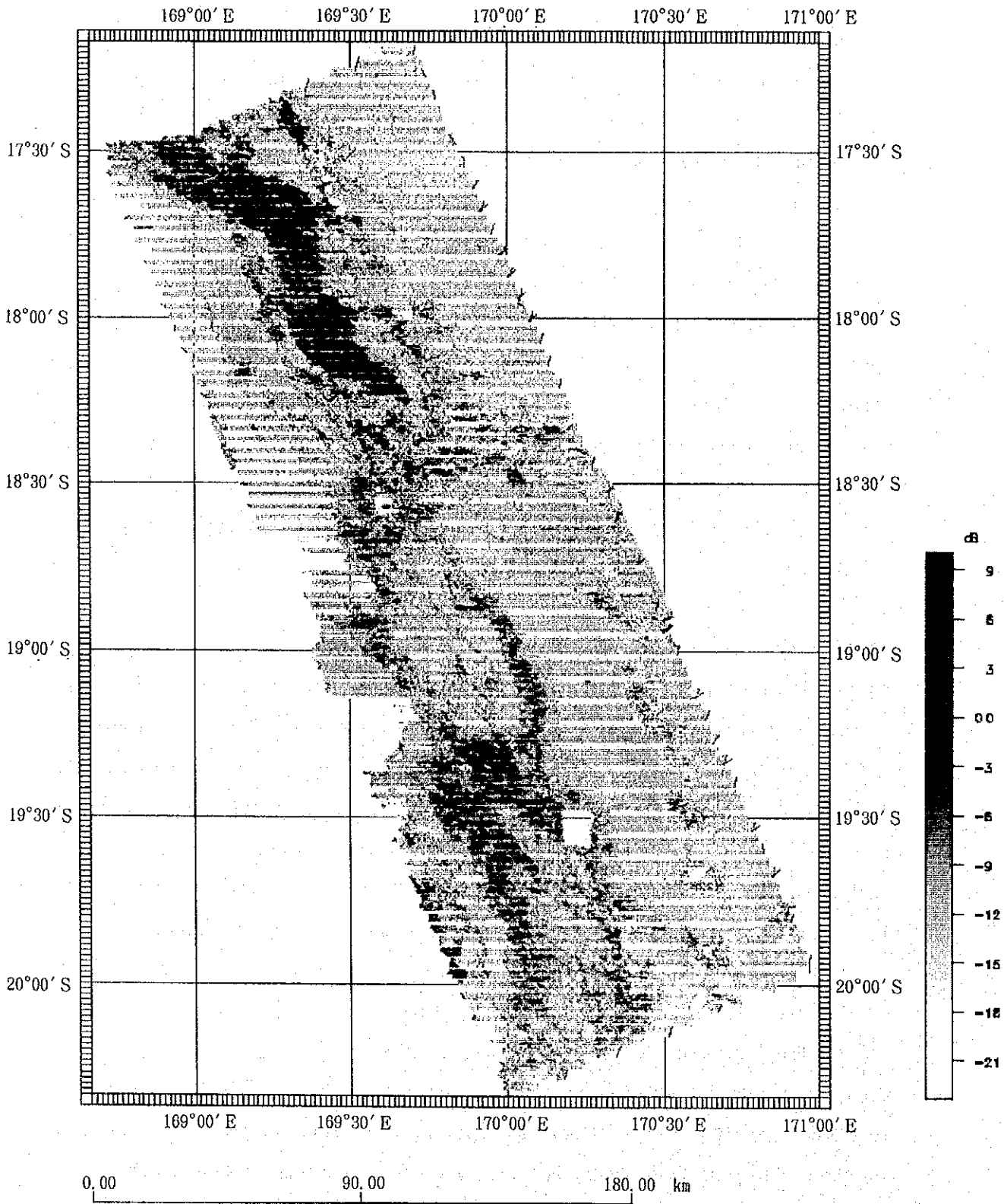


Figure 3-4-2-1 Sound Pressure Images Based on MBES

masses existing in some rises on the slopes and the bottom of the trough.

Distribution of sediments and rock masses is as follows; Sediments are distributed extensively on the western slopes of the trough that constitute an arc platform and on the eastern slopes that connects to the North Fiji Basin, except some areas in the southwestern part adjacent to Tunna Island and Anaton Island where volcanic activity is brisk.

Rock masses thinly covered with sediments are distributed extensively on the bottom of the Trough in the north. There is uneven submarine topography in shoals between the Vate Trough and the Erromango Trough, and outcrops are distributed at random. Sediments are extensively distributed on the bottom of the Erromango Basin. Thick sediments, with the smallest irregularities within the survey area, are distributed on depressions in the eastern part of the basin floor. Some parts of the ridge-shaped rise showed relatively strong reflection, and distribution of outcrops here was identified by FDC.

Shoals between the Erromango Basin and the Futuna Trough showed the strongest reflection among the survey area, indicating the existence of outcrops. Places showing relatively darker shades around the above-mentioned shoals and to the northern part of the Futuna Trough, especially on the western slopes, indicate the existence of rock masses thinly covered with sediments.

Sediments in the southern part of the Futuna Trough become slightly thicker than in the northern part but the records become lighter shades. Rock masses on slopes and the areas adjacent to them are covered with sediments.

(3) Sub-bottom Profiling

Use of SBP for the EPR hydrothermal deposit survey was suspended because variations of sea-floors reflection would become greater than those of penetrated reflection due to vehement changes of submarine topography in the hydrothermal deposits survey area. As the nSBP unit which was installed last year, had a narrower beam angle (4°) than that of the conventional type, we performed sub-bottom profiling during this survey cruising with the object of identifying applicability of this unit for the back-arc basin survey.

Figures 3-4-3 (1), (2) show some examples of sub-bottom profiling records. In these cases, we performed the sub-bottom profiling with a view to identifying the thickness of sediments covering rock masses, sedimentary structure and faults.

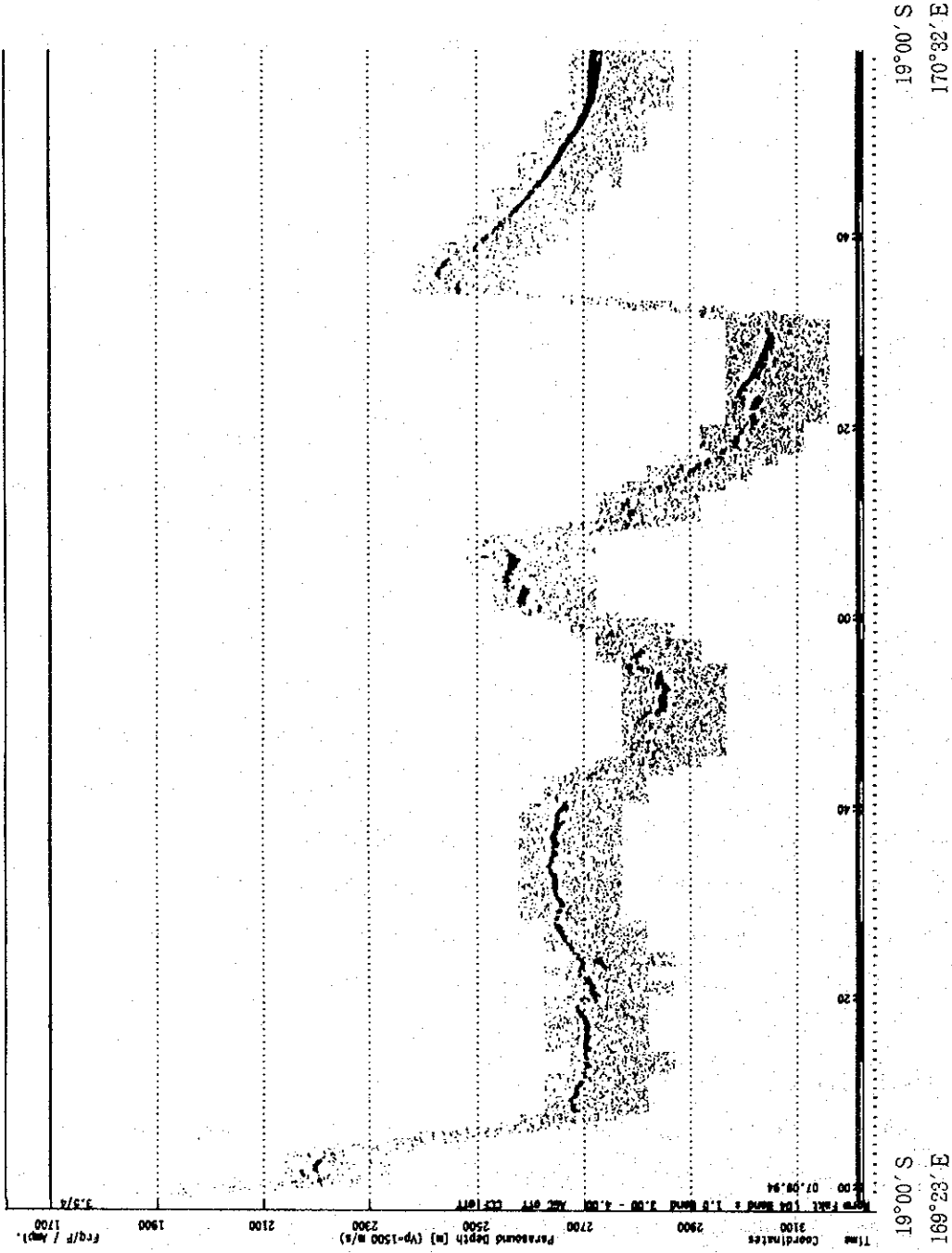
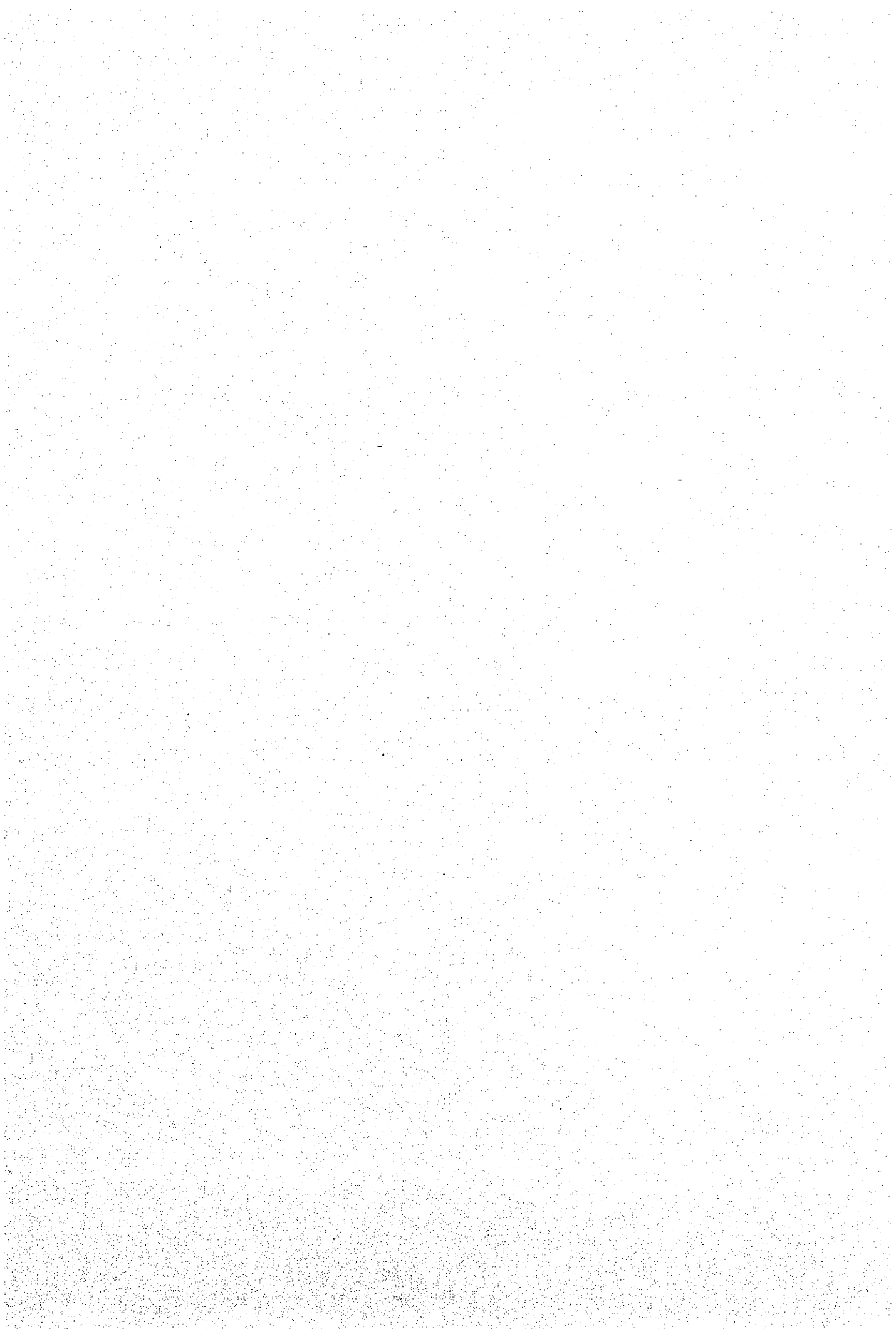


Figure 3-4-3 SBP Profile (1)
 area : Errromango Basin
 Line No. 55-0-0



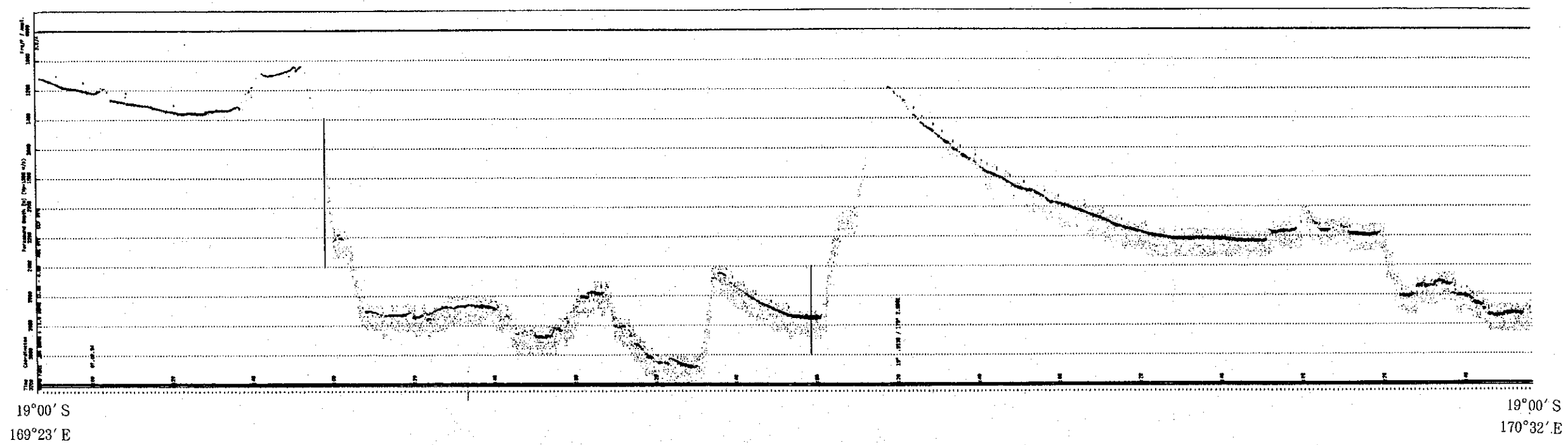
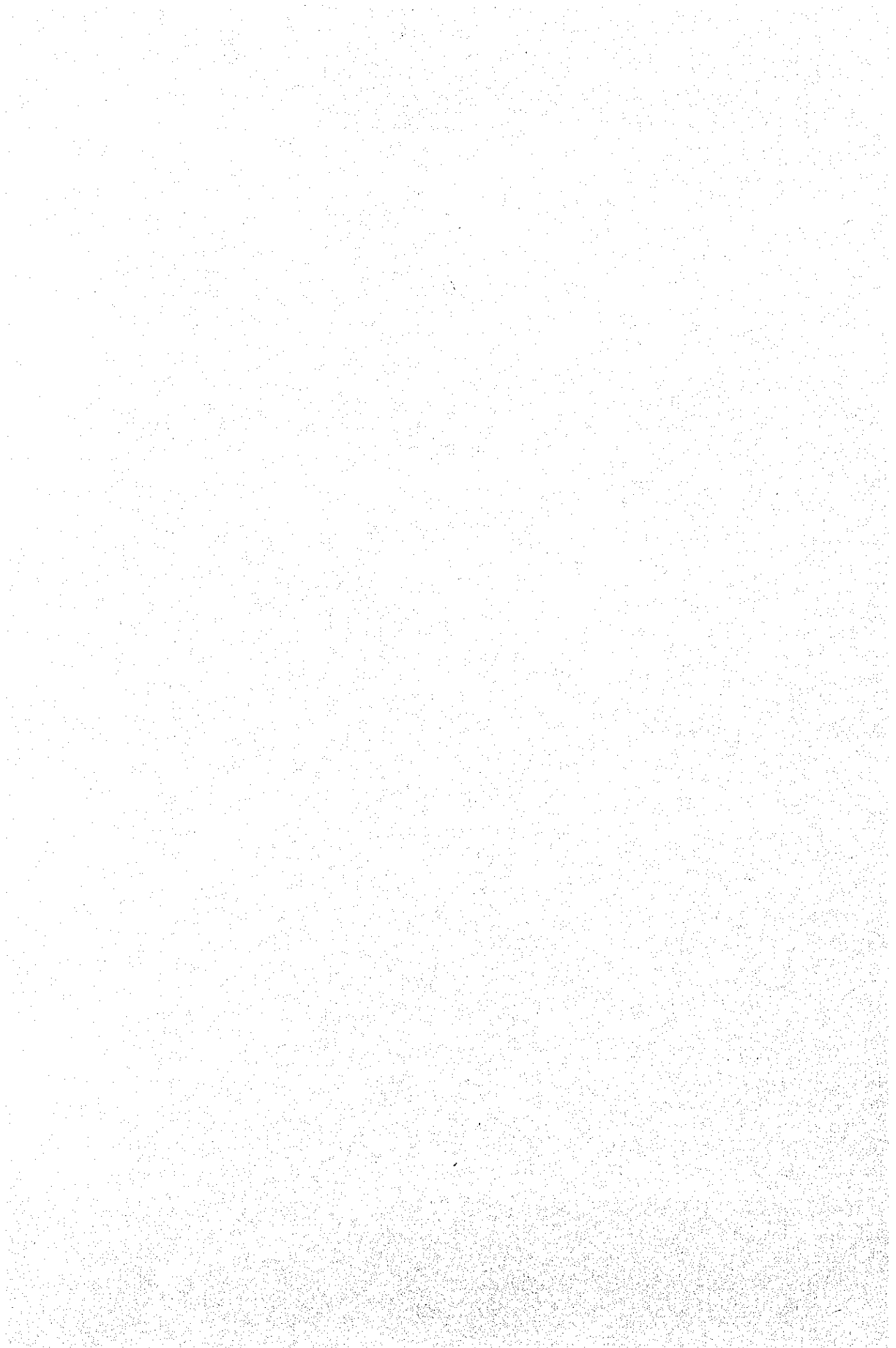


Figure 3-4-3 SBP Profile (2)
 area : Erromango Basin
 Line No. 55-0-0



We found that sub-bottom profiling by nSBP offered the advantage of

- high monolayer resolution for identifying sedimentary structures of turbidite and others,

but also exhibits problems such as

- low penetration against sediments of pyroclastic materials (its maximum is only 20-25m).
- weaker reflection signals as inclinations of submarine topography become bigger. It is not clear whether the reflection signal becomes weaker because of the existence of sedimentary layers or because of the influence of the inclinations.
- difficulty in determining the border between sediments and rock masses when sedimentary layers are thin and rock masses exist right under the sedimentary layers due to shortage of penetration and effect of inclinations.

Using SBP for hydrothermal deposit survey is not effective for determining of outcrops because the variation of surface shapes is great and said variation causes lowering of sound pressure.

Layer thickness was not clear because the entire penetration was insufficient. A tendency, however, that layer thickness increases as the depth increases or layer thickness is thicker on the east than on the west is obtained from the facts that the layer thickness on the west, near the volcanic arc as its depth becomes shallower, is as thin as 5m and on the east, the area across the back arc basin to the North Fiji Basin where the depth becomes deeper, is as thick as 10m. Variations of the thickness of sedimentary layers between the north and south or between different basins are not clear.